Dynamic capillarity in heterogeneous media with discontinuous capillary pressure

Hoeksema, J.

Award date:
2015

Dynamic capillarity in heterogeneous media with discontinuous capillary pressure

Jasper Hoeksema
Technical University Eindhoven
Supervisor: dr. S. Pop

December 17, 2014

Abstract

We present an extension of the interface conditions for the non-equilibrium model of capillary pressure, and investigate both the behaviour at and around these interfaces. First we explore the merits of proving the non-equilibrium conditions via a regularization approach, and investigate the relation between the dynamic and equilibrium model at the interface when the evolution of the saturation on one side is given. Next, we simulate the flow over an entire interval, and show scaling and critical behaviour for the dynamic parameter τ.

Contents

1 Introduction

The phenomenon of the flow of water through porous media like sand or certain type of rock has sparked man's interest for thousands of years, and has been thoroughly studied for the last two centuries. There is a host of applications, for example the engineering of filters, oil recovery, and more recently, the sequestration of CO2. Often these are systems where multiple, mostly immiscible, phases are present. For example, in petroleum engineering the interaction between water, steam and oil plays a pivotal role. Moreover, one often encounters heterogenous porous media, where the characteristics of the rock rapidly changes. As is the case in, for example, fractured media like shale rock.

For our research we will restrict ourselves however to two phases. Models for two-phase flow usually assume a so called equilibrium model, where the capillary pressure is only dependent on the saturation. This is however not always accurate. For example, in filtration processes measured capillary pressure deviates significantly from this theoretical assumption, as noted in [2]. For the past decade certain modifications, like a dynamic effect where the capillary pressure is also dependent on the rate of change of the saturation, have been intensively studied, for example in [2].

Most of this research focuses on a continuous capillary pressure over the material interface, like [6]. Loosening this restriction, even in the equilibrium case, can show some very interesting behaviour, as shown in [3]. In the case for periodic but vanishingly small heterogeneities this can even lead to the trapping of oil, for example the trapping of oil, as shown with a homogenization approach in [4] and [5]. The conjunction of these two, a discontinuous and dynamic capillary pressure, is however not yet extensively studied. In this article we will try to make a modest starting point, to instigate further analysis.

2 Two-phase flow in homogenous media

2.1 Porous Media

A porous medium consists of a solid substance, such as rock, containing a huge number of interconnected small voids, called pores. These pores are filled with one or multiple fluids, usually referred to as phases, for example oil, gas, water or steam. In a two-phase system one of the phases is denoted as the *wetting phase* and the other as the *non-wetting phase*, based on which phase tends to cover most of the pores' surfaces, such as shown in Figure 1.

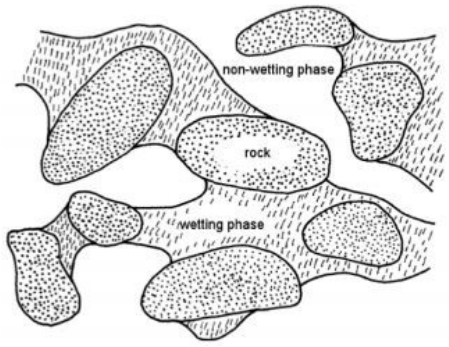

Figure 1: A cross-section of a porous medium

Whereas the structure of a porous medium can be highly irregular on the scale of these pores, on a large enough scale the flow through the porous medium can be approximated as homogeneous proces. This scale is called the Representative Element Volume scale. At this REV-scale, we can describe certain averaged properties and the relationships between these properties. Therefore, before the mathematical model for two-phase flow will be introduced, a few of these properties specific to porous materials and their interrelationships will be listed.

- *porosity* (Φ) [-] is a material parameter, denoting the fraction of the volume of all the voids over the total volume of rock and pores combined.
- *saturation* (s_i) [-], the fraction of the void filled by phase i
- *capillary pressure* (p_c) [Pa] is the pressure difference between the wetting (with pressure p_w) and the non-wetting phase (with pressure p_n), due to the interfacial tension between the curved surfaces involved

Several models have been derived, both theoretically and experimentally, to express the dynamic relationship between flow, capillary pressure, and saturation.

- *Fluid balance*
  The familiar fluid balance equation can be accommodated for flow in porous media. With q_i [m s] being the flow of phase i, it is as follows:

$$\phi \frac{\partial s_i}{\partial t} + \frac{\partial q_i}{\partial x} = 0 \qquad i = w, n \tag{1}$$

- *Darcy's law*
  Darcy's law states that the flow q_i is proportional to the variation of p_i, with proportionality constant λ_i, called the mobility of phase i. In other words, with x [m] denoting position, the following relationship holds:

$$q_i + \lambda_i \frac{\partial p_i}{\partial x} = 0 \qquad i = w, n \tag{2}$$

However, in order to distinguish between material/fluid parameters and parameters that are dependent on saturation, the mobility λ_i is defined as:

$$\lambda_i = \frac{k k_{ri}}{\mu_i} \tag{3}$$

Here k [m^2] is the absolute permeability of the porous medium, and k_{ri} [-] and μ_i [Pa s] the relative permeability and viscosity of phase i. Both the relative permeability and the capillary pressure are assumed to be solely dependent on the saturation, as seen below.

- *Capillary pressure*

The relation between capillary pressure and saturation is often described by the Leverett-model. With σ [Pa m] being the interfacial tension between the two phases and J a so-called Leverett function, the capillary pressure is:

$$p_c = p_n - p_w = \sigma \sqrt{\frac{\phi}{k} J(s_w)} \tag{4}$$

In the Brooks-Corey model, J is approximated by a power function.

$$J(s) \quad = \quad s^{-1/\lambda_1} \qquad\qquad \textit{(Brooks-Corey)} \tag{5}$$

Various modifications to (4) have been suggested. In this article we consider the one proposed by Hassanizadeh and Gray, as mentioned and used in [2].

$$p_c = p_n - p_w = \sigma \sqrt{\frac{\phi}{k}} J(s_w) - \tau \frac{\partial s_w}{\partial t} \tag{6}$$

Where $\tau > 0$ [Pa s] is a damping factor.

- *Relative permeability*

Several models exist. According to the Burdine model it holds that:

$$\begin{aligned} k_{rw}(s) &= s^{\frac{2+3\lambda_2}{\lambda_2}} \qquad\qquad \textit{(Burdine)} \\ k_{rn}(s) &= (1-s)^2 \left(1 - s^{\frac{2+\lambda_2}{\lambda_2}}\right) \end{aligned}$$

2.2 Model Equations

We assume that the flow is one-dimensional and horizontal, so that gravitational effects can be disregarded. Furthermore, we assume that the medium is saturated, so that $s_w + s_n = 1$, where s_w is the saturation of the wetting fluid, and s_n is the saturation of the non-wetting fluid.

Note that, since $s_w + s_n = 1$, it is easy to see from **(1)** that the total flow $q = q_w + q_n$ is constant in space. Therefore it is possible to express q_w in terms of q and p_c. Namely, rewrite equation **(2)** and subtract to get p_c, as seen below. Additionally, it is assumed that the total flow q is also constant over time.

$$\begin{aligned} \frac{q_i}{\lambda_i} &= -\frac{\partial p_i}{\partial x} \\ \frac{q_w}{\lambda_w} - \frac{q_n}{\lambda_n} &= \frac{\partial p_n}{\partial x} - \frac{\partial p_w}{\partial x} \\ \frac{q_w}{\lambda_w} - \frac{q - q_w}{\lambda_n} &= \frac{\partial p_c}{\partial x} \end{aligned}$$

Next, rearrange terms to derive q_w.

$$\begin{aligned} q_w(\frac{1}{\lambda_w} + \frac{1}{\lambda_n}) &= \frac{\partial p_c}{\partial x} + \frac{q}{\lambda_n} \\ q_w &= \frac{\lambda_w}{\lambda_n + \lambda_w} q + \frac{\lambda_n \lambda_w}{\lambda_n + \lambda_w} \frac{\partial p_c}{\partial x} \end{aligned} \tag{7}$$

Finally, substituting **(7)** into equation **(1)** for the water phase and using the definition for mobility and capillary pressure, a non-linear convection-diffusion equation is found for s_w:

$$\begin{aligned} \phi \frac{\partial s_w}{\partial t} + \frac{\partial}{\partial x}\left(q \frac{\lambda_w}{\lambda_w + \lambda_n} + \frac{\lambda_w \lambda_n}{\lambda_w + \lambda_n} \frac{\partial}{\partial x} p_c \right) &= 0 \\ \phi \frac{\partial s_w}{\partial t} + \frac{\partial}{\partial x}\left(q \frac{\mu_n k_{rw}}{\mu_n k_{rw} + \mu_w k_{rn}} + k \frac{k_{rn} k_{rw}}{\mu_n k_{rw} + \mu_w k_{rn}} \frac{\partial}{\partial x}\left[\sigma \sqrt{\frac{\phi}{k}} J(s_w) - \tau \frac{\partial s_w}{\partial t} \right] \right) &= 0 \\ \phi \frac{\partial s_w}{\partial t} + \frac{\partial}{\partial x}\left(q \frac{k_{rw}}{k_{rw} + \frac{\mu_w}{\mu_n} k_{rn}} + \frac{k}{\mu_n} \frac{k_{rn} k_{rw}}{k_{rw} + \frac{\mu_w}{\mu_n} k_{rn}} \frac{\partial}{\partial x}\left[\sigma \sqrt{\frac{\phi}{k}} J(s_w) - \tau \frac{\partial s_w}{\partial t} \right] \right) &= 0 \end{aligned} \tag{8}$$

Now, let L be a characteristic length, and let the dimensionless quantities $\hat{t}, \hat{x}, \hat{k}, \hat{\tau}$ be defined as follows:

$$\hat{t} := \frac{q}{L} t, \quad \hat{x} := \frac{x}{L}, \quad \hat{k} := \frac{k}{L^2}, \quad \hat{\tau} = \frac{q}{\sigma} \tau \tag{9}$$

Moreover, let $s = s_w$. Then by writing in terms of **(9)**, and dividing by $\frac{q}{L}$, equation **(8)** can be expressed in dimensionless form, as shown below. Note that both $\frac{\partial q}{\partial x}$ and $\frac{\partial q}{\partial t}$ are equal to zero.

$$\begin{aligned} \frac{q\phi}{L} \frac{\partial s}{\partial \hat{t}} + \frac{1}{L} \frac{\partial}{\partial \hat{x}}\left(q \frac{k_{rw}}{k_{rw} + \frac{\mu_w}{\mu_n} k_{rn}} + \frac{L^2 \hat{k}}{\mu_n} \frac{k_{rn} k_{rw}}{k_{rw} + \frac{\mu_w}{\mu_n} k_{rn}} \frac{1}{L} \frac{\partial}{\partial x}\left[\sigma \sqrt{\frac{\phi}{L^2 \hat{k}}} J(s) - \frac{\sigma \hat{\tau}}{q} \frac{\partial s}{\partial t} \right] \right) &= 0 \\ \phi \frac{\partial s}{\partial \hat{t}} + \frac{\partial}{\partial \hat{x}}\left(\frac{k_{rw}}{k_{rw} + \frac{\mu_w}{\mu_n} k_{rn}} + \left(\frac{\hat{\sigma}}{q \mu_n} \right) \hat{k} \frac{k_{rn} k_{rw}}{k_{rw} + \frac{\mu_w}{\mu_n} k_{rn}} \frac{\partial}{\partial \hat{x}}\left[\sqrt{\frac{\phi}{\hat{k}}} J(s) - \hat{\tau} \frac{\partial s}{\partial \hat{t}} \right] \right) &= 0 \end{aligned} \tag{10}$$

For simplicity, define the dimensionless mobility M and capillary number N_c by

$$\begin{aligned} M &= \mu_n/\mu_w \\ N_c &= \frac{\sigma}{q\mu_n} \end{aligned}$$

Moreover, introduce the dimensionless functions of the wetting phase, the flux F and fractional flow function $f_w(s)$:

$$f_w(s) = \frac{k_{rw}(s)}{k_{rw}(s) + \frac{k_{rn}(s)}{M}} \tag{11}$$

$$F = f_w(s) + k\bar{\lambda}(s)\frac{\partial}{\partial x}\left(\sqrt{\frac{\phi}{k}}J(s) - \tau\frac{\partial s}{\partial t}\right) \tag{12}$$

Finally, let the mobility $\bar{\lambda}$ be defined as $\bar{\lambda}(s) = N_c k_{rn}(s) f_w(s)$. Then **(10)** can be written as

$$\phi\frac{\partial s}{\partial t} + \frac{\partial F}{\partial x} = 0 \tag{13}$$

Different substitutions beside **(9)** result different forms, and different conventions for both the capillary number N_c and damping factor τ. This is especially important when the capillary number is extremely small, reducing the relative contribution of the diffusion and damping term, allowing for the use of limit techniques. For example, in order to use the homogenization techniques shown in [4] and [5]. In this case it also becomes necessary to rewrite the damping term so as to isolate the contribution of the vanishing capillary number, as used in [2]. However, these techniques and considerations are beyond the scope of this article, and therefore the current convention is used, with an eye on simplicity.

3 Heterogenous media

In equation (13) and we assumed that both the porosity ϕ and absolute permeability k were constant. However, as mentioned before, in real-life applications one often encounters heterogeneities, for example in fractured media. In this article we will model these heterogeneities by letting $\phi(x)$ and $k(x)$ be dependent on x, but piece-wise constant. At the interfaces between this otherwise homogeneous media, where there are discontinuities in $\phi(x)$ and $k(x)$, certain boundary conditions are needed. This approach is based on [3].

First note that because there are no sinks or sources beside those at infinity, conservation of flow through this interfaces means the flux must be continuous. Secondly, one could argue that the capillary pressure must be continuous too. However, this runs into problems when $J(1) \neq 0$, as is in our case. For example, consider the capillary pressure in the equilibrium model, for two porous media with different characteristics.

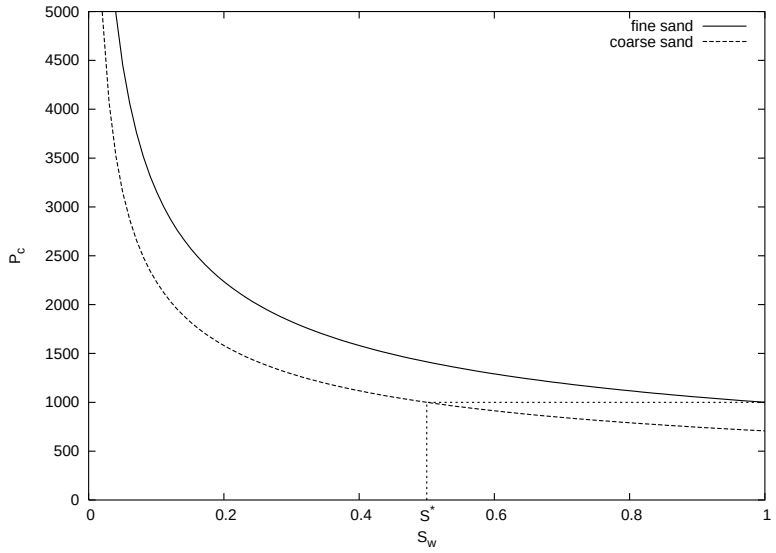

Figure 2: Capillary pressure in coarse and fine sand, as a function of saturation

From Figure 2 it is apparent that if $s > s^*$ for the lower curve, continuous capillary pressure is impossible. However, one could expect that in this case the saturation of the upper curve remains at $s = 1$. Under certain circumstances this is exactly what happens, as shown in [3] and proven with a regularization approach. In this section we will summarize the results from [3], adapt them to the case of non-equilibrium capillary pressure, and identify key obstacles that arise in using the regularization approach to the non-equilibrium case.

3.1 Equilibrium Interface Conditions

We assume that the discontinuity is at $x = 0$, and that the functions $k(x)$ and $\phi(x)$ are piecewise constant. Note that since this section concerns the equilibrium case, $\tau(x) = 0$ for all x. Now, let $h(x) = \sqrt{\frac{k(x)}{\phi(x)}}$, then

$$h(x) = \begin{cases} h^-, & \text{if} \quad x < 0, \\ h^+, & \text{if} \quad x > 0. \end{cases} \tag{14}$$

Additionally, let us use the following notation for any arbitrary function f over s and x:

$$\begin{aligned} f(s, x \uparrow 0) &= f^- \\ f(s, x \downarrow 0) &= f^+ \\ [f] &= f^+ - f^- \end{aligned}$$

Now, suppose $h^- > h^+$. Since $\tau(x) = 0$ let us consider only the static term p_s of the capillary pressure p_c, as used in the dimensionless equation (21), so that $p_s(s, x) = \frac{J(s)}{h(x)}$. Moreover, we introduce the maximal saturation s^*, as defined by:

$$\frac{J(s^*)}{h^-} = \frac{J(1)}{h^+} \tag{15}$$

The maximal saturation can be seen as the highest possible saturation s^- while still maintaining continuity of the capillary pressure over the interface, i.e. $p_s^- = p_s^+$. Also note that since $h^- > h^+$ the quantity s^* is well defined. Now, the so called extended pressure condition, as described in [3], is as follows

Theorem 1. Extended Pressure Condition - Equilibrium Model
Suppose $h^- > h^+$. Then

$$\begin{aligned} \tfrac{J(s^+)}{h^+} &= \tfrac{J(s^-)}{h^-}, && \textit{if} \quad s^- \le s^*, \\ s^+ &= 1, && \textit{if} \quad s^- > s^*. \end{aligned} \tag{16}$$

This corresponds the intuitive notion apparent from Figure 2. The formal proof is based on regularization, however, we will omit these details for simplicity. Note that the capillary pressure is continuous, i.e. $p_s^- = p_s^+$ whenever $s^+ < 1$, and if $s^+ = 1$ it must be that $s^- \ge s^*$. Therefore, we can write the extended pressure condition as follows:

Corollary 1. *Suppose $h^- > h^+$. Then $(s^+ - 1)[p_s] = 0$, and $[p_s] \ge 0$.*

This form of writing the pressure condition was used in [4].

Finally, to setup the comparison with the non-equilibrium case, we introduce the static threshold pressure $\bar{p}_s(x)$, the lowest possible capillary pressure in the equilibrium case. It is defined by

$$\bar{p}_s = p_s(1, x) = \frac{J(1)}{h(x)} \tag{17}$$

Note that in Figure 2 the values of $\bar{p}_s$ for different values of h correspond to the intersections of the curves with the vertical line $s = 1$, and since $h^- > h^+$ it must hold that $\bar{p}_s^- < \bar{p}_s^+$.

3.2 Non-Equilibrium Interface Conditions

When the capillary pressure is not solely dependent on s the extended pressure condition is not apparent. However, we can modify it to achieve something similar. For example, as in the previous section, let us fix t and consider the dynamic capillary pressure p_c, as used in the flux-equation **(12)**, with $p_c(x,t) = \frac{J(s)}{h(x)} - \tau(x)s_t$, where $s_t = \frac{\partial s}{\partial t}$. Now suppose we fix the term s_t. Then, dependent on $\tau^+ s_t^+$ and $\tau^- s_t^-$, a possible relation between s and p_c^-, p_c^+ is illustrated in Figure 3.

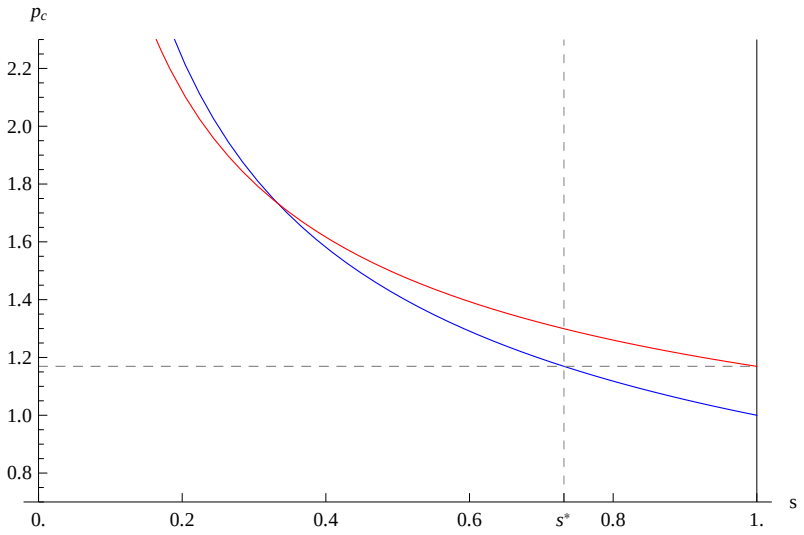

Figure 3: Capillary pressure in a non-equilibrium case

The difference between Figure 2 and 3 is clear: possible intersections of the two different curves can exist, and $h^- > h^+$ does not guarantee the difference in threshold pressure. However, we can use the same line of reasoning as in the non-equilibrium model. In order to do so, let us use the notation of the previous section and introduce the dynamic threshold pressure $\bar{p}_c$, as defined by

$$\bar{p}_c(x,t) = \frac{J(1)}{h(x)} - \tau(x)s_t \tag{18}$$

Note that $\bar{p}_s$ is independent of both s and s_t and therefore a characteristic of the material itself, whereas $\bar{p}_c$ is not. Now, in light of Corollary 1 and Figure 3 we can state the following conjecture.

Conjecture 1. Extended Pressure Condition - Non-Equilibrium Model
If $[\bar{p}_c] \geq 0$ *it holds that* $(s^+ - 1)[p_c] = 0$, *and if* $[\bar{p}_c] \leq 0$ *it holds that* $(s^- - 1)[p_c] = 0$. *Moreover,* $[\bar{p}_c][p_c] \geq 0$.

Note that when $\tau^- = \tau^+ = 0$ and $h^- > h^+$ Conjecture 1 is equivalent to Corollary 1.

Now, let us introduce both the left and right maximal saturations, similar to the equilibrium case:

$$\begin{aligned} \frac{J(1)}{h^-} &= \frac{J(s_+^*(t))}{h^+} - [\tau s_t] \\ \frac{J(s_-^*(t))}{h^-} &= \frac{J(1)}{h^+} - [\tau s_t] \end{aligned}$$

Note that these are not necessarily well-defined if $J(s)$ is only defined on the domain $[0,1]$. However, as will be shown below, this is irrelevant for our purpose. Now, using the maximal

saturations, we can rewrite Conjecture 1 to derive a more general version of Theorem 1. However, in our notation of $s^{\pm}(t)$, $s^{*}_{\pm}(t)$ and $p^{\pm}_{c}(t)$, we try to stress that these are also functions of time and not just the material parameters, in contrast to p_s, although in the proof and in further sections this will be omitted for convenience.

Theorem 2. Boundary Conditions

Suppose Conjecture 1 holds. Assume $h^- > h^+$.

Then, depending on $[\tau s_t](t)$, for any t exactly one of the following three conditions hold:

(i) $[\tau s_t](t) > [\bar{p}_s]$, *in which case it holds that*

$$\begin{aligned} p_c^-(t) &= p_c^+(t) && \text{iff} \quad s^+(t) \le s^*_+(t), \\ s^-(t) &= 1, && \text{if} \quad s^+(t) > s^*_+(t). \end{aligned}$$

(ii) $[\tau s_t](t) = [\bar{p}_s]$

$p_c(t)$ *is continuous, regardless of* $s^+(t)$ *or* $s^-(t)$.

(iii) $[\tau s_t](t) < [\bar{p}_s]$, *in which case it holds that*

$$\begin{aligned} p_c^-(t) &= p_c^+(t) && \text{iff} \quad s^-(t) \le s^*_-(t), \\ s^+(t) &= 1, && \text{if} \quad s^-(t) > s^*_-(t). \end{aligned}$$

Note that $[\bar{p}_s] > 0$ when $J(1) \neq 0$, and therefore the standard case in [3] with $\tau = 0$ (and therefore $[\tau s_t] = 0$) is a special case of condition **(iii)** above.

Proof. First note that $[\bar{p}_c] = [\bar{p}_s] - [\tau s_t]$, and therefore the conditions **(i)**, **(ii)** and **(iii)** simply correspond to the cases $[\bar{p}_c] < 0$, $[\bar{p}_c] = 0$, and $[\bar{p}_c] > 0$.

Moreover, let us rewrite the definition of s^*_+ and s^*_- as follows:

$$\begin{aligned} \frac{J(s^*_+) - J(1)}{h^+} &= -[\bar{p}_c] \\ \frac{J(s^*_-) - J(1)}{h^-} &= [\bar{p}_c] \end{aligned}$$

It is clear that either $s^*_+ < 1$, $s^*_- = s^*_+ = 1$, or $s^*_- < 1$, corresponding to the conditions **(i)**, **(ii)** and **(iii)**. Since s^*_+ is only used in condition **(i)**, and s^*_- only used in condition **(iii)**, s^*_+ and s^*_- are well defined.

Now, let us suppose that condition **(i)** is satisfied, i.e. $[\tau s_t] > [\bar{p}_s]$, and therefore $s^*_+ < 1$. According to Conjecture 1 p_c is continuous if both $s^+ < 1$ and $s^- < 1$. Moreover, $p_c^- \ge p_c^+$, which can be rewritten as

$$\begin{aligned} \frac{J(s^-)}{h^-} &\ge \frac{J(s^+)}{h^+} - [\tau s_t] \\ \frac{J(s^-)}{h^-} &\ge \frac{J(s^+) - J(s^*_+)}{h^+} + \frac{J(s^*_+)}{h^+} - [\tau s_t] \\ \frac{J(s^-) - J(1)}{h^-} &\ge \frac{J(s^+) - J(s^*_+)}{h^+} \end{aligned} \tag{19}$$

It follows that if $s^+ < s^*_+$, then $s^- < 1$. If $s^+ = s^*_+$, p_c must be continuous. To see this, assume p_c is discontinuous. Then $s^- = 1$ according to Conjecture 1, and by definition of s^*_+, p_c is continuous. Therefore it follows that if $s^+ \le s^*_+$, p_c is continuous.

On the other hand, if p_c is continuous, (19) becomes an equality, and because $s^- \leq 1$ it follows that $s^+ \leq s^*_+$. This means that if $s^+ > s^*_+$, p_c must be discontinuous, in which case according to Conjecture 1 $s^- = 1$. Our result for condition **(i)** is now proven. Proofs for conditions **(ii)** and **(iii)** are similar.

□

An attentive reader could note that the inequalities that determine either $s^+ = 1$ or $s^- = 1$ - and therefore would possibly imply $s^+_t = 0$ or $s^-_t = 0$ - also depend on s^+_t and s^-_t themselves, and could start to wonder if this could lead to circular reasoning if not all variables were treated as given. In situation (**iii**) for example, it is obvious multiple s^- exist when $s^+ = 1$, but the proof of Theorem 1 does not explicitly disallow two s^+_t's to exist when all others are given - one in the continuous case $s^- \leq s^*_-$ (note again that s^*_- is dependent on s^+_t), and one in the discontinuous case with $s^- > s^*_-$. However, a quick calculation would show that if $s^+_t > 0$ is such that $s^- > s^*_-$, this would imply that $s^- > s^*_-$ would still hold when $s_t = 0$, and moreover $[\bar{p}_c]|_{s^+_t=0} > [\bar{p}_c]|_{s^+_t>0} > 0$, so that the sign of $[\bar{p}_c]$ does not switch. Note that this also implies that whenever s^+ would hit the 'wall' $s^+ = 1$ with a positive speed s^+_t, reverting to $s^+_t = 0$ would not suddenly make the system switch to one with continuous pressure. Also note that we are now talking about the *uniqueness* of either $s^+(t)$ or $s^-(t)$. For more on this subject, see Section 4.1, where this phenomenon is studied, among other.

3.3 Regularization Approach

We already noted that the non-equilibrium variant of Theorem 2, Theorem 1, was rigourously proven through a regularization approach in [3]. So while Conjecture 1 was based on the same intuitive concept as used in the non-equilibrium boundary conditions, we will now consequently show the merits of the regularization approach. However, our efforts were not conclusive, and therefore we will restrict ourselves to providing partial results and outlining key ideas that could be helpful in further research.

As before, let F be written in terms of **(12)**, and let $k(x)$, $\phi(x)$ and $\tau(x)$ be all dependent on x. Moreover, substitute $h(x)$ for $\frac{k(x)}{\phi(x)}$, and thus

$$F = f_w(s) + \phi(x)h^2(x)\bar{\lambda}(s)\frac{\partial}{\partial x}\left(\frac{J(s)}{h(x)} - \tau(x)s_t\right) \tag{20}$$

We will approximate the discontinuous functions ϕ, h and τ by the smooth monotone functions ϕ_ϵ, h_ϵ, and τ_ϵ, with the regularization parameter $\epsilon > 0$, such that they only differ on a very small interval $[-\epsilon, \epsilon]$ around the discontinuity at $x = 0$. The values $s(-\epsilon)$, $s_t(-\epsilon)$, $s(\epsilon)$ and $s_t(\epsilon)$ will correspond to s^-, s_t^-, s^+ and s_t^+, and as we will let $\epsilon \to 0$, we will derive a relation between these values.

Now let ϕ_ϵ, h_ϵ and τ_ϵ on the interval $[-\epsilon, \epsilon]$ be defined as $\phi_\epsilon(x) = \hat{\phi}(\frac{x}{\epsilon})$, $h_\epsilon(x) = \hat{h}(\frac{x}{\epsilon})$, and $\tau_\epsilon(x) = \hat{\tau}(\frac{x}{\epsilon})$ where $\hat{\phi}$, $\hat{h}$ and $\hat{\tau}$ are smooth and monotone on the interval $[-1, 1]$. We will denote the flux on this regularized problem as F_ϵ, with s_ϵ and $s_{t,\epsilon}$ its solution. Finally, let us map the interval $[-\epsilon, \epsilon]$ to $[-1, 1]$ by defining y as $y = \frac{x}{\epsilon}$, $v_\epsilon(y) = s_\epsilon(x)$ (and $v_{t,\epsilon}(y)$ correspondingly). Then we can rewrite **(20)** as follows:

$$F_\epsilon = f_w(v_\epsilon) + \frac{1}{\epsilon}\hat{\phi}(y)\hat{h}^2(y)\bar{\lambda}(v_\epsilon)\frac{\partial}{\partial y}\left(\frac{J(v_\epsilon)}{\hat{h}(y)} - \hat{\tau}(y)v_{t,\epsilon}\right) \tag{21}$$

Now, assume that the saturation v_ϵ, $0 \le v_\epsilon \le 1$, converges as $\epsilon \downarrow 0$ towards a limit function v, and moreover assume that during this limit process the flux remains bounded, uniformly in ϵ. Then the limit function v satisfies

$$\bar{\lambda}(v)\frac{\partial}{\partial x}\left(\frac{J(v)}{\hat{h}(y)} - \hat{\tau}(y)v_t\right) = 0 \quad \text{for} -1 < y < 1 \tag{22}$$

Here $v(y)$ and $v_t(y)$ are assumed piecewise smooth. In the equilibrium case, when $\tau(x) = 0$ for all x, then **(22)** leads to a relation between $v(-1)$ and $v(+1)$, and therefore between s^- and s^+. The key in this reasoning is that the differential equation **(22)** only admits monotone solutions $v(y)$ and $p_c(y)$. In our case however, this is not as straightforward, as we will see later below. First we will consider equation **(21)** more closely to illicit more information about $v(y)$ and $p_c(y)$ beside condition **(22)**.

Note that since $\frac{1}{\epsilon}\frac{\partial F_\epsilon}{\partial y} = \frac{\partial F_\epsilon}{\partial x} = -v_{t,\epsilon}$, we have $\frac{\partial F}{\partial y} = 0$ for the limit flux $F = \lim_{\epsilon \to 0} F_\epsilon$, and therefore $F = F_0$ for a certain F_0. This represents the familiar flux condition, $F^- = F^+$. We can use this to show that $p_c(y)$ is monotone except for the case where $F = 1$.

Lemma 1.
Let $F_0 = F^- = F^+$, and suppose $F_0 \neq 1$, and that $p_c(y)$ is smooth. Then $p_c(y)$ is monotone. Moreover, $(F_0 - 1)[p_c] \ge 0$.

Note that while the sign of $[p_c]$ can be determined in this case, the question if discontinuities in pressure only arise when either s^+ or s^- are equal to one, i.e. $(s^+ - 1)[p_c]$ or $(s^- - 1)[p_c]$, is not answered.

Proof. Equation **(21)** tells us

$$F_0 = \lim_{\epsilon \to 0} f_w(v_\epsilon) + \lim_{\epsilon \to 0} \frac{1}{\epsilon} \hat{\phi}(y) \hat{h}^2(y) \bar{\lambda}(v_\epsilon) \frac{\partial p_{c,\epsilon}}{\partial y} \tag{23}$$

Consider only those points y^* where $\frac{\partial p_c}{\partial y} \neq 0$, and therefore $v(y^*) = 1$. Then, for small enough ϵ we can state that

$$\begin{aligned}
(F_0 - 1) &= \lim_{\epsilon \to 0} \frac{1}{\epsilon} \hat{\phi}(y) \hat{h}^2(y) \bar{\lambda}(v_\epsilon) \frac{\partial p_{c,\epsilon}}{\partial y} \\
\text{sign}(F_0 - 1) &= \text{sign}\left(\frac{1}{\epsilon} \hat{\phi}(y) \hat{h}^2(y) \bar{\lambda}(v_\epsilon) \frac{\partial p_{c,\epsilon}}{\partial y} \right) \\
\text{sign}(F_0 - 1) &= \text{sign}\left(\frac{\partial p_{c,\epsilon}}{\partial y} \right)
\end{aligned}$$

Therefore, $\frac{\partial p_c}{\partial y}$, the limit of $\frac{\partial p_{c,\epsilon}}{\partial y}$, must either be 0 or have the same sign as $(F_0 - 1)$. Our result easily follows. □

From the proof it's clear that its not just a statement about the possible monotonicity of p_c but also of the behaviour of the function $p_{c,\epsilon}$ for small enough ϵ. This can be important even when there is no immediate connection to its limit, p_c. One could spit for more hints by considering not just F_ϵ but also $\frac{\partial}{\partial y} F_\epsilon$ or $\frac{\partial^2}{\partial y^2} F_\epsilon$ and contemplating convexity or concavity of the relevant functions, taking into account the behaviour of f, λ, ϕ,h and the boundedness of v. However without more advanced expertise in regularisation and the behaviour of functions like $p_{c,\epsilon}$ as they converge this leads to a maze of even more unsatisfying answers, and therefore we relegate this subject to future research.

Still, it is possible to illustrate why the local behaviour or the shape of $p_c(y)$ or $p_{c,e}(y)$ near the points where $v(y) = 1$ matters. In the following examples we will provide sufficient conditions for Conjecture 1 based on this notion.

Lemma 2. *Suppose that $p_c(y)$ is convex. Then Conjecture 1 holds.*

Proof. Let us first consider the case where $s^- < 1$ and $s^+ < 1$. Suppose $[p_c] \neq 0$, then it follows from equation (22) and the continuity of $v(y)$ that there exists a, b such that $v(y) < 1$ for all $y \notin [a, b]$, and $v(y) = 1$ for all $y \in [a, a + \epsilon_1)$ and $y \in (b - \epsilon_2, b]$, for certain positive ϵ_1, ϵ_2. Moreover, $p_c(-1) = p_c(a)$ and $p_c(1) = p(b)$. However, there exists no convex solution $p_c(y)$ such that $p_c(a) \neq p_c(b)$. Therefore $p_c(-1) = p_c(1)$, which contradicts with our assumption. Therefore, if $s^- < 1$ and $s^+ < 1$, it holds that $[p_c] = 0$.

Now suppose $s^- < 1$, but $s^+ = 1$. From our previous reasoning we can conclude that there exist a and b such that $v(y) < 1$ and $\frac{\partial p_c}{\partial y} = 0$ for all $y \in [-1, a)$, and $v(y) = 1$ for all $y \in [b, 1]$. But convexity of p_c now implies that $p(1) \geq p(a)$. Therefore, $[p_c] \geq 0$. The case for $s^- = 1$ and $s^+ < 1$ is similar. □

Note that Lemma 2 and the fact that $\frac{\partial p_c}{\partial y} = 0$ when $v(y) < 1$ imply the following.

Corollary 2. *Suppose that p_c is smooth, and $\frac{\partial^2 p_c}{\partial y^2} \geq 0$ for all y^* such that $v(y) = 1$. Then Conjecture 1 holds.*

As noted, apparently the behaviour of $p_c(y^*)$ around the points where $v(y^*) = 1$ is important, i.e. the threshold pressure $\bar{p}_c$. One can even prove a stronger version of Corollary 2, regarding the monotonicity of $\bar{p}_c$.

Lemma 3. *Suppose that for all y^* such that $v(y^*) = 1$, there exists an $\epsilon > 0$ such that the threshold pressure $\bar{p}_c(y)$ is strictly increasing for all $y \in (y^* - \epsilon, y^* + \epsilon)$. Then Conjecture 1 holds, with $[p_c] \geq 0$. Similarly, if $\bar{p}_c(y)$ is strictly decreasing on these neighborhoods, Conjecture 1 holds, with $[p_c] \leq 0$.*

Note that in the equilibrium case where $\bar{p}_c = \frac{J(1)}{h(y)}$, $\bar{p}_c(y)$ is strictly monotone on the entire interval [-1,1], but also note that Lemma 3 does not require strict monotonicity of $\bar{p}_c(y)$ on the entire interval [-1,1].

Proof. Equation (22) states that either $\frac{\partial p_c}{\partial y} = 0$, or $\bar{\lambda}(v) = 0$, in which case either $v = 0$ or $v = 1$. Now suppose that for all y^* such that $v(y^*) = 1$, $\bar{p}_c(y^*)$ is strictly increasing on at least one open neighborhood of y^*. Since $\bar{p}_c$ is piecewise smooth, this means that both left and right derivatives exist and are positive: $\frac{\partial \bar{p}_c}{\partial y}|_{y\uparrow\downarrow y^*} > 0$. Then we can write, omitting the side of the derivative for convenience,

$$\begin{aligned}
\left.\frac{\partial p_c}{\partial y}\right|_{y^*} &= \left.\frac{\partial}{\partial y}\left(\frac{J(v)}{\hat{h}(y)} - \hat{\tau}(y)v_t(y)\right)\right|_{y^*} \\
&= \left.\left(\frac{J'(1)}{\hat{h}(y^*)}\frac{\partial v}{\partial y} - \frac{J(1)}{\hat{h}(y^*)^2}\frac{\partial h}{\partial y} - \frac{\partial}{\partial y}\left(\hat{\tau}(y)v_t(y)\right)\right)\right|_{y^*} \\
&= \left.\frac{\partial \bar{p}_c}{\partial y}\right|_{y^*} + \left.\frac{J'(1)}{\hat{h}(y^*)}\frac{\partial v}{\partial y}\right|_{y^*}
\end{aligned}$$

Now if $\frac{\partial p_c}{\partial y}|_{y^*} = 0$, it follows that $\frac{\partial \bar{p}_c}{\partial y}|_{y^*}$ and $\frac{\partial v}{\partial y}|_{y^*}$ have the same sign, since $J'(v) < 0$ for $\forall v$. Therefore, it holds that $\frac{\partial v}{\partial y}|_{y^*} > 0$ for all y^* such that $v(y^*) = 1$ and $\frac{\partial p_c}{\partial y}|_{y^*} = 0$, allowing only increasing solutions for $\frac{\partial p_c}{\partial y}|_{y^*} = 0$. This means that $v(y) = 1$ for all $y \geq y^*$, for any y^*, and therefore $s^+ = v(1) = 1$.

On the other hand, suppose $\frac{\partial p_c}{\partial y}|_{y^*} \neq 0$. Piecewise smoothness of v now requires $\frac{\partial v}{\partial y}|_{y^*} = 0$, forcing $\frac{\partial p_c}{\partial y}|_{y^*} > 0$. Therefore we can conclude that $(s^+ - 1)[p_c] = 1$, and $[p_c] \geq 0$, and our result follows. The case for $\bar{p}_c(y^*)$ strictly decreasing is similar.

□

Note that in our boundary conditions we did not place any restrictions on the sign of $[\bar{p}_c]$, as it was possible to have either way, while in the non-equilibrium case this is equal to the sign of -$[h]$. However, even in the non/equilibrium case it is easy to imagine scenarios where the sign of $[\bar{p}_c]$ is still tied directly to -$[h]$. For example, suppose $[h] < 0$ (and therefore $h(y)$ strictly decreasing, and that v_t is both smooth with respect to y as to t on those points where $v = 1$. Then $v_t = 0$ and $\frac{\partial v_t}{\partial y}|_{v=1} = 0$, thus we get $\frac{\partial \bar{p}_c}{\partial y}|_{v=1} > 0$, and because of Lemma 3, Conjecture 1 holds with $[\bar{p}_c] > 0$.

The problem is that this smoothness in t is not guaranteed, and with the results about non-smooth travelling waves referenced in [2] in mind, maybe not even expected. Since the relation between v_t and $\frac{\partial v_t}{\partial y}$ depends on the limiting behavior of F_ϵ v_t it is very possible $v(t)$ behaves very differently from $s(t)$, causing $v_t \neq 0$ on parts with $v = 1$, or to have free boundaries with infinite speed, or even possibly undefined.

Again, more knowledge about regularisation processes would be needed to resolve these questions. Possible avenues for further study could involve more information and bounds on the converging behaviour of both v_ϵ and $v_{t,\epsilon}$ (and its effect on F, p_c and λ), a case-by-case analysis of the possible shapes that $(\phi h^2 \lambda \frac{\partial}{\partial y} p_c)$ could take, and as noted, thorough research on regularisation. While it is very possible that this knowledge is available, it does however fall beyond the scope of this article. Therefore, in further sections, we explore the possibilities in the case Conjecture 1 is true.

4 Analysis behaviour Non-Equilibrium Pressure Condition

In the previous section we posited certain interface conditions in the non-equilibrium model. In this section however, we will try to study not its possible proof, but its consequences. Instead of an inequality and a one-to-one relation between s^- and s^+, the interface conditions now dictate an inequality and a differential equation between $s^-(t)$ and $s^+(t)$, leading to myriad differences.

Still, we will show the existence and uniqueness of either $s^+(t)$ or $s^-(t)$ in certain circumstances, and confirm the intuitive notion of the equilibrium model as a time-limit of the non-equilibrium model. Next, restricting one of $s^-(t)$ or $s^+(t)$ to be monotone, we will study the ordering between the non-equilibrium $s(t)$ and its equilibrium counterpart. Moreover, we will model the interface conditions for given $s^-(t)$ and a certain set of material characteristics, in order to illustrate and validate our results, and even illicit more questions.

4.1 Equilibrium States

The extended pressure condition presupposes s_t is defined for all t. This does not necessarily mean s_t is continuous in t, for example, whenever $s^+(t)$ reaches 1 and the inequality part of the extended pressure condition kicks in, it is possible that $s_t^+(t)$ will suddenly change if we impose no other restrictions. However, in order to relate $s^-(t)$ and $s^+(t)$ to their physical equivalents, we can expect $s^-(t)$ and $s^+(t)$ to be continuous, and for $s_t^-(t)$ and $s_t^+(t)$ to have at most countable discontinuities. Therefore, in this and all following sections, we will suppose that $s^-(t)$ and $s^+(t)$ are piecewise smooth in t. Moreover, $s_t^-(t)$ and $s_t^+(t)$ will be defined in a neighborhood to the right of t.

Now, let us first consider under which circumstances either $s^+(t)$ or $s^-(t)$ is uniquely determined by the other.

Theorem 3. Existence and uniqueness
Suppose Conjecture 1 holds. Furthermore, suppose $[p_c] \geq 0$ *for* $\forall t$ *with* $t_0 < t < t_e$. *Then* $s^+(t)$ *is uniquely determined by* $s^-(t)$, *for all* t *in the interval* $[t_0, t_e]$. *Similarly, if* $[p_c] \leq 0$ *for all* $t > t_0$, *then* $s^-(t)$ *is uniquely determined by* $s^+(t)$.

Note that whenever $s^-(t) < 1$ (respectively $s^+(t) < 1$) for all t, $[p_c] \geq 0$ (respectively $[p_c] \leq 0$) is guaranteed according to Conjecture 1, and thus is a special case of Theorem 3.

Proof. If $[p_c] \geq 0$ for all t in the interval $[t_0, t_e]$, then according to the proof of Theorem 2 only the scenario's **(ii)** and **(iii)** are allowed. Therefore, either $[p_c] = 0$ or $s^+ = 1$ and $s^- > s_-^*$ (note that this also implies that $s^+(t)$ can only be non-smooth whenever $s^-(t)$ is non-smooth or $s^+(t) = 1$). This last statement can be rephrased as $\frac{J(s^-)}{h^-} - \tau^- s_t^- < \frac{J(1)}{h^+} - \tau^+ s_t^+$.

Now, consider the interval $[t_0, t_1)$ where $t_1 \leq t_e$ and such that both $s^-(t)$ and $s^+(t)$ are smooth for $t < t_1$, and therefore such that $[p_c](t)$ is continuous for $t < t_1$. Furthermore, define $G_1(s^+, t)$ as

$$G_1(s^+, t) \quad = \quad \frac{1}{\tau^+}\left(\frac{J(s^+)}{h^+} - \frac{J(s^-(t))}{h^-} + \tau^- s_t^-(t)\right) \tag{24}$$

The suffix (t) from $s^+(t)$ is removed, in order to clarify that the pressure condition now dictates a ODE in s^+, whereas $s^-(t)$ is considered as given. Now we can state that either $[p_c] = 0$, in which case $s_t^+ = G_1(s^+, t)$, or $[p_c] \neq 0$, in which case $s^+ = 1$ and $s_t^+ < G_1(s^+, t)$. However, if $G_1(s^+, t) \leq 0$, then $s_t < 0$ whenever $[p_c] \neq 0$, meaning $s^+ < 1$ in a neighbourhood to the right of t. But since $[p_c]$ is continuous on the interval $[t_0, t_1)$, this is impossible. Therefore, we can write s_t as follows:

$$\begin{array}{rll} s_t^+ = G_1(s^+, t) & \text{if} & s^+ < 1 \textit{ or } G_1(s^+, t) \leq 0 \\ = G_2(s^+, t) & \text{if} & s^+ = 1 \textit{ and } G_1(s^+, t) > 0 \end{array} \tag{25}$$

Where $G_1(s^+, t)$ is defined as before, and $G_2(s^+, t) = 0$. Note that the conditions ($s^+ < 1$ *or* $G_1(s^+, t) \leq 0$) and ($s^+ = 1$ *and* $G_1(s^+, t) > 0$) exclude each other, and therefore (25) is well-defined. Now, since $s^-(t)$ is smooth both $G_1(s^+, t)$ and $G_2(s^+, t)$ are continuous in t and continuously differentiable in s^+, so for both the ODE's $s_t^+ = G_1(s^+, t)$ and $s_t^+ = G_2(s^+, t)$ there exist unique and smooth solutions.

Now, consider the full interval $[t_0, t_e]$. Then since s^+ is continuous, one can string together multiple intervals $[t_0, t_1)$, $[t_1, t_2)$, and so on, where for every i it holds that at $t = t_i$ either $s^+ = 1$ or the smoothness of $s^-(t)$ is broken, and either $s_t^+ = G_1(s^+, t)$ for the entire interval $[t_i, t_{i+1})$ or $s_t^+ = G_2(s^+, t)$. This way we have created an unique and continuous, but not necessarily smooth, solution $s^+(t)$ for our original problem. The case for $[p_c] \leq 0$ is similar. □

Note that we have now proven, as a special case, that whenever $s^- < 1$, s^+ is uniquely determined in our non-equilibrium model, the same as in the equilibrium model. In the latter s^+ is only a function of s^-, or to be precise $s^+ = s_e^+$ with $\frac{J(s_e^+)}{h^+} = \max\left(\frac{J(s^-)}{h^-}, \frac{J(1)}{h^+}\right)$. In the former we also have to take s_t^- and s_t^+ into account. However, the quantity s_e^+ still plays an important role, and we will see that it can be considered as an asymptotically stable equilibrium state of the ODE defining $s^+(t)$.

Theorem 4. Stability
Suppose Conjecture 1 holds. Furthermore, suppose $s_t^-(t) = 0$ *for all* $t > t_0$*, that* $s^- < 1$*, and let* s_e^+ *be defined by* $\frac{J(s_e^+)}{h^+} = \max\left(\frac{J(s^-)}{h^-}, \frac{J(1)}{h^+}\right)$.
Then $s^+ = s_e^+$ *is a stable equilibrium. Moreover,* $s_t^+(t)(s^+(t) - s_e^+) < 0$ *and* $(s^+(0) - s_e^+)(s^+(t) - s_e^+) > 0$ *whenever* $s^+(t) \neq s_e^+$.

Proof. Since $s^- < 1$, we can conclude that $[p_c] \geq 0$. Moreover, since $s_t^- = 0$, $G_1(s^+, t)$ is now only dependent on s^+ and s^-:

$$G_1(s^+) = \frac{1}{\tau^+}\left(\frac{J(s^+)}{h^+} - \frac{J(s^-)}{h^-}\right)$$

Now, suppose $\frac{J(s_e^+)}{h^+} = \frac{J(s^-)}{h^-}$. Then we can simplify $G_1(s^+)$ even further

$$G_1(s^+) = \frac{J(s^+) - J(s_e^+)}{h^+\tau^+} \tag{26}$$

But since $G_1(1) = \frac{J(1) - J(s_e^+)}{h^+\tau^+} \leq 0$, equation (25) states that $s_t^+ = G_1(s^+)$ for all s^+. One can even deduce stability directly, since we can now linearize (25) as follows:

$$\begin{aligned}\frac{\partial}{\partial s^+} G_1(s^+)\big|_{s_e^+} &= \frac{\partial}{\partial s^+}\frac{1}{\tau^+}\left(\frac{J(s^+)}{h^+} - \frac{J(s^-)}{h^-}\right)\Bigg|_{s_e^+} \\ &= \frac{J'(s_e^+)}{\tau^+ h^+}\end{aligned}$$

Since $J'(s) < 0$ for all s, s_e is a stable equilibrium. Moreover, since $s_t = G_1(s^+)$ defines a autonomous ODE, solutions do not cross. However, since $s^+(t) = s_e^+$ is a possible solution, it follows that $s^+(t)$ does not cross s_e. Our results now easily follow.

Now, suppose $\frac{J(1)}{h^+} > \frac{J(s^-)}{h^-}$, which gives $s_e^+ = 1$. Then for all $s^+ < 1$ it holds that

$$\begin{aligned}s_t^+ &= \frac{J(s^+)}{h^+\tau^+} - \frac{J(s^-)}{h^-\tau^+} \\ &> \frac{J(s^+) - J(s_e^+)}{h^+\tau^+} > 0\end{aligned}$$

Since $s_t^+ = 0$ only when $s^+ = s_e^+$, both stability of s_e and the rest of our results easily follow.

□

Note that the last part of the theorem states that not only that s_e^+ is a stable equilibrium, but also that $s^+(t)$ will never pass s_e^+. It is also clear from the proof that a lower τ guarantees a more rapid decay of s^+ to its equilibrium-model counterpart s_e^+, validating in this specific case the notion that dynamic models with decreasing τ should more and more resemble the equilibrium model.

Remark 1. *In Theorem 4 the condition $s^- < 1$ was needed to ensure uniqueness of s^+. However, even when that is not the case we can sometimes say something about s^+.*

For example, suppose $s^- = 1$, and $h^- = h^+$, and therefore $s_e = 1$. Then we can write the boundary condition $[p_c] \leq 0$ as follows:

$$\begin{aligned} \frac{J(1)}{h} &\geq \frac{J(s^+)}{h} - \tau^+ s_t^+ \\ s_t^+ &\geq \frac{J(s^+) - J(1)}{\tau^+ h} \end{aligned}$$

But this means that for every $s^+ < 1$, its derivative $s_t^+ > 0$, and therefore the equilibrium point $s_e = 1$ is stable.

Also note that this reasoning can not be used when $h^- \neq h^+$, cause in that case either there are multiple equilibria points, or since when $s_e^+ < 1$ stability is not guaranteed. It is possible however to derive a similar bound to s_t^+, in this case:

$$\begin{aligned} \frac{J(1)}{h} &\geq \frac{J(s^+)}{h} - \tau^+ s_t^+ \\ s_t^+ &\geq \frac{J(s^+)}{\tau^+ h^+} - \frac{J(1)}{\tau^- h^-} \end{aligned}$$

In Theorem 4 we noticed that $s^+(t)$ converges to an equilibrium state when $s^-(t)$ is constant. However, as we will see below, we can make an ever stronger statement, concerning the case where $s^-(t)$ has a limit state as well.

Theorem 5. Asymptotic Limit
Suppose Conjecture 1 holds. Furthermore, suppose $s^-(t) < 1$ for all $t > t_0$, and that $\lim_{t\to\infty} s^-(t) = s_e^-$ and $\lim_{t\to\infty} s_t^-(t) = 0$. Now let s_e^+ be defined by $\frac{J(s_e^+)}{h^+} = \max\left(\frac{J(s_e^-)}{h^-}, \frac{J(1)}{h^+}\right)$.
Then $\lim_{t\to\infty} s^+(t) = s_e^+$.

Proof. As before, it holds that $[p_c] \geq 0$ for all t since $s^-(t) < 1$ for all t. Now, suppose $\frac{J(s_e^+)}{h^+} = \frac{J(s_e^-)}{h^-}$ and $s_e^+ < 1$. Then we can write $G_1(s^+, t)$ in terms of s_e^+ and s_e^-. Namely, define $\epsilon_1(t) = \left(\frac{J(s_e^-) - J(s^-)}{\tau^+ h^-} - \frac{\tau^-}{\tau^+} s_t^-\right)$, then:

$$\begin{aligned} G_1(s^+, t) &= \frac{1}{\tau^+}\left(\frac{J(s^+(t)) - J(s_e^+)}{h^+} - \frac{J(s^-(t)) - J(s_e^-)}{h^-} + \tau^- s_t^-(t)\right) \\ &= \frac{J(s^+(t)) - J(s_e^+)}{\tau^+ h^+} + \left(\frac{J(s_e^-) - J(s^-(t))}{\tau^+ h^-} - \frac{\tau^-}{\tau^+} s_t^-(t)\right) \\ &= \frac{J(s^+(t)) - J(s_e^+)}{\tau^+ h^+} + \epsilon_1(t) \end{aligned}$$

Now, since $\lim_{t\to\infty} s^-(t) = s_e^-$ and $\lim_{t\to\infty} s_t^-(t) = 0$, it follows that $\lim_{t\to\infty} \epsilon_1(t) = 0$. But then, since $s_e < 1$, there exists a t^* such that whenever $t > t^*$, it holds that $G_1(1, t) = \frac{J(1) - J(s_e^+)}{h^+\tau^+} + \epsilon_1(t) < 0$. But in this case, equation (25) states that $s_t^+ = G_1(s^+)$ for all s^+ when $t > t^*$. Now, define the function $\epsilon_2(t)$ such that $(J(s_e^+) + \tau^+ h^+ \epsilon_1(t)) = J(s_e^+ + \epsilon_2(t))$. It is clear that $\epsilon_2(t)$ and $\epsilon_1(t)$ have opposite signs, and $\lim_{t\to\infty} \epsilon_2(t) = 0$. Then

$$\begin{aligned} s_t^+ &= \frac{J(s^+) - J(s_e^+)}{\tau^+ h^+} + \epsilon_1(t) \\ &= \frac{J(s^+) - J(s_e^+ + \epsilon_2(t))}{\tau^+ h^+} \end{aligned}$$

So whenever $s^+ > s_e^+ + \epsilon_2(t)$, $s_t^+ < 0$, when $s^+ = s_e^+ + \epsilon_2(t)$, $s_t^+ = 0$, and when $s^+ < s_e^+ + \epsilon_2(t)$, $s_t^+ > 0$. Therefore, $(s_e^+ + \epsilon_2(t))$ can be seen as a moving attractor of the ODE defining $s^+(t)$. However, since $\lim_{t\to\infty} \epsilon_2(t) = 0$, it follows that $\lim_{t\to\infty} s^+(t) = s_e^+$.

The case for $s_e^+ = 1$ and $\frac{J(1)}{h^+} = \frac{J(s_e^-)}{h^-}$ can be seen as an extension, since whenever $G_1(s^+, t) \leq 0$ the previous arguments apply, and when $G_1(s^+, t) > 0$, it follows that $s^+ = 1$ and $s_t^+ = 0$. In both cases $\lim_{t\to\infty} s^+ = 1$.

Finally, suppose $s_e = 1$ and $\frac{J(1)}{h^+} > \frac{J(s_e^-)}{h^-}$. Then since $\lim_{t\to\infty} s^-(t) = s_e^-$ and $\lim_{t\to\infty} s_t^-(t) = 0$ there is a t^* such that when $t > t^*$ and $s^+ < 1$ it holds that

$$\begin{aligned} s_t^+ &= \frac{J(s^+)}{h^+\tau^+} - \frac{J(s^-)}{h^-\tau^+} + \frac{\tau^-}{\tau^+} s_t^- \\ &> \frac{J(s^+) - J(1)}{h^+\tau^+} > 0 \end{aligned}$$

Our results now easily follow.

□

It is clear that $s^+(t)$ seems to converge to its equilibrium model counterpart s_e^+ whenever either s_t^- or the quantities τ^- and τ^+ become vanishingly small. However we would also like to make qualitative statements about the relation between the time-dependent equilibrium state $s_e^+(t)$ and $s^+(t)$, which occurs when $\tau^- s_t^-$ is not that small. As we will see in the next two sections that is indeed possible, but we will have to restrict ourselves to two special cases: one where $[h] = 0$, and one where $[\tau] = 0$. We would also like to note that because of the central role of the quantity $[\tau s_t]$ in Theorem 2, we will use somewhat cumbersome notations like $\frac{\partial}{\partial t}[\tau s_t]$ instead of $[\tau s_{t,t}]$ or $[\tau s]_{t,t}$.

4.2 Pure τ-heterogeneities

Similar to the static s_e^+, defined by $\frac{J(s_e^+)}{h^+} = \max\left(\frac{J(s_e^-)}{h^-}, \frac{J(1)}{h^+}\right)$ with $\lim_{t\to\infty} s^-(t) = s_e^-$, we will introduce the time-dependent quantities $s_e^+(t)$ and $s_e^-(t)$, which in the case of no restrictions on $[\tau]$ or $[h]$ will be defined by

$$\begin{aligned}\frac{J(s_e^+(t))}{h^+} &= \max\left(\frac{J(s^-(t))}{h^-}, \frac{J(1)}{h^+}\right)\\ \frac{J(s_e^-(t))}{h^+} &= \max\left(\frac{J(s^+(t))}{h^+}, \frac{J(1)}{h^-}\right)\end{aligned}$$

It is obvious that, given $s^-(t)$, $s_e^+(t)$ simply denotes the value s^+ would take when at time t the quantities τ^+ and τ^- would suddenly be set to zero, corresponding to the equilibrium model.

Now, in this section we will study the relation between $s_e^+(t)$ and $s^+(t)$ when the heterogeneities consist of τ-heterogeneities only, so when $[h] = 0$. Note that in this case it follows that simply $s_e^+(t) = s^-(t)$. The first two results concern the case where $s^+(t) = s_e^+(t)$ at a certain time t.

Lemma 4.
Suppose Conjecture 1 holds. Furthermore, suppose $\tau^- > \tau^+$, $h^+ = h^-$, $s^+, s^- < 1$ *and that* $(s_t^-)^2 + (s_t^+)^2 \neq 0$. *Then, if* $s^+ = s^-$ *it holds that* $s_t^+ s_t^- > 0$, *and that* $|s_t^+| > |s_t^-|$. *Moreover,* $s_t^-\left(\frac{\partial}{\partial t}[\tau s_t]\right) < 0$.

Note that these last two conditions mean that $s^-(t)$ can never catch up with $s^+(t)$ - only the other way around - and that whenever it does, the sign of $[\tau s_t](t)$ changes.

Alternatively, one can imagine that when the saturations on both sides of the τ-heterogeneity are similar and changes are small, the one on the side with the smaller τ seems to 'lag' the other one. However, this notion of $s^-(t)$ as an delayed version of $s^+(t)$ is incorrect when $s^+(t) \neq s^-(t)$ and $s_t^+(t)$ is not that small. For example, since s_t^- is a monotone function of s_t^+ when all other variables remain constant, it follows that a rapid enough change of sign in $s_t^+(t)$ incurs a similar rapid change in $s_t^-(t)$, without $s^-(t)$ first catching up with $s^+(t)$.

Proof. Suppose $s^+{=}s^-$ and $s^+, s^- < 1$, and therefore $[p_c] = 0$. Then we can rewrite the pressure condition as $\tau^+ s_t^+ = \tau^- s_t^-$. It is clear both s_t^+ and s_t^- have the same sign, and since $\tau^- > \tau^+$ it follows that $|s_t^+| > |s_t^-|$. Now since $s^+ > s^-$, $s^+ = s^-$, and $s^+ < s^-$ correspond to the cases $[\tau s_t] > 0$, $[\tau s_t] = 0$ and $[\tau s_t] < 0$ our last result follows too. One can also derive this directly, by

$$\begin{aligned}\frac{\partial}{\partial t}[\tau s_t]\Big|_{s^+=s^-} &= \frac{1}{h}\frac{\partial}{\partial t}\left(J(s^+) - J(s^-)\right)\Big|_{s^+=s^-}\\ &= \frac{1}{h}\left(J'(s^+)s_t^+ - J'(s^-)s_t^-\right)\big|_{s^+=s^-}\\ &= \frac{J'(s^-)}{h}\left(\frac{\tau^-}{\tau^+} - 1\right)s_t^- \qquad (27)\end{aligned}$$

Since $J'(s) < 0$ for all s and $\tau^- > \tau^+$, our last result follows.

□

We can see in the above proof that the sign of $[\tau s_t](t)$ is directly related to the position of s^+ (or alternatively, s^-) relative to its equilibrium counterpart. Moreover, since $\left(\frac{1}{h^+} - \frac{1}{h^-}\right) = 0$, the sign of $[\tau s_t](t)$ corresponds inversely to the sign of $[\bar{p}_c]$. As we will show in Theorem 6, this connection also allows us to establish which side uniquely determines the other for all $t > t_0$, when certain conditions are met. But first, we state a similar result as Lemma 4, now concerning the case where $s_t^- = 0$.

Lemma 5.
Suppose Conjecture 1 *holds, and that* $s_t^- = s_t^+ = 0$, $s^- = s^+ < 1$, $h^- = h^+$, *and* $\tau^- > \tau^+$. *Then if either* $\frac{\partial^2 s^-}{\partial t^2}$ *or* $\frac{\partial^2 s^+}{\partial t^2}$ *are unequal to zero, it holds that* $\frac{\partial^2 s^+}{\partial t^2}\frac{\partial^2 s^-}{\partial t^2} > 0$, $|\frac{\partial^2 s^+}{\partial t^2}| > |\frac{\partial^2 s^-}{\partial t^2}|$, $\frac{\partial}{\partial t}[\tau s_t] = 0$, *and* $\frac{\partial^2 s^-}{\partial t^2}\left(\frac{\partial^2}{\partial t^2}[\tau s_t]\right) < 0$.

Proof. From (27) we can see that when $s_t^- = 0$, it follows that $\tau^+\frac{\partial^2 s^+}{\partial t^2} = \tau^-\frac{\partial^2 s^-}{\partial t^2}$, and the first part of our theorem follows. Moreover, we can write

$$\begin{aligned}\frac{\partial^2}{\partial t^2}[\tau s_t] &= \frac{1}{h}\frac{\partial^2}{\partial t^2}\left(J(s^+) - J(s^-)\right) \\ &= \frac{1}{h}\left(J'(s^+)\frac{\partial^2}{\partial t^2}s^+ - J'(s^-)\frac{\partial^2}{\partial t^2}s^-\right) + \frac{1}{h}\left(J''(s^+)(s_t^+)^2 - J''(s^-)(s_t^-)^2\right) \quad (28)\end{aligned}$$

But since $s_t^- = s_t^+ = 0$ and $s^- = s^+$ we can use our previous result to conclude that

$$\begin{aligned}\frac{\partial^2}{\partial t^2}[\tau s_t] &= \frac{1}{h}\left(J'(s^+)\frac{\partial^2}{\partial t^2}s^+ - J'(s^-)\frac{\partial^2}{\partial t^2}s^-\right) \\ &= \frac{J'(s^-)}{h}\left(\frac{\tau^-}{\tau^+} - 1\right)\frac{\partial^2}{\partial t^2}s^- \quad (29)\end{aligned}$$

And our result follows. □

Whereas Lemma 4 stated that $s^-(t)$ could never catch up with $s^+(t)$, only the other way around, Lemma 5 states that when $s^+(t)$ *starts* up from an equilibrium position at time t_0, i.e. $s^+(t_0) = s^-(t_0)$ and $s_t^+ = 0$, $s^+(t)$ will outrun $s^-(t)$. Now, armed with these two Lemma's we can make statements about the relative position of $s^+(t)$ or $s^-(t)$ and their equilibrium counterparts for áll $t > t_0$, whenever one side is strictly monotone in t, as we will see in the final result of this section.

Theorem 6.
Suppose $\tau^- > \tau^+$, $s_t^-(t_0) = s_t^+(t_0) = 0$ *and* $s^+(t_0) = s^-(t_0)$.
Furthermore, suppose $\frac{\partial s_t^-(t)}{\partial t}|_{t=t_0} > 0$, *and either* $s_t^-(t) > 0$, $s^-(t) < 1$ *for all* $t > t_0$, *or* $s_t^+(t) > 0$, $s^+(t) < 1$ *for all* $t > t_0$. *Then* $s^+(t) > s^-(t)$ *and* $[\bar{p}_c] > 0$ *for all* $t > t_0$.
Similarly, suppose $\frac{\partial s_t^-(t)}{\partial t}|_{t=t_0} < 0$, *and either* $s_t^-(t) < 0$, $s^-(t) < 1$ *for all* $t > t_0$, *or* $s_t^+(t) < 0$, $s^+(t) < 1$ *for all* $t > t_0$. *It holds that* $s^+(t) < s^-(t)$ *and* $[\bar{p}_c] < 0$ *for all* $t > t_0$.

Proof. Suppose $\frac{\partial s_t^-(t)}{\partial t}|_{t=t_0} > 0$, and $s_t^-(t) > 0$, $s^-(t) < 1$ for all t. (The proofs for the cases $\frac{\partial s_t^-(t)}{\partial t}|_{t=t_0} > 0$ e.a. are similar to the one below.)

Now, according to Lemma 5 and the definition of t_0, it holds that $\frac{\partial s_t^+(t)}{\partial t}|_{t=t_0} > \frac{\partial s_t^-(t)}{\partial t}|_{t=t_0} > 0$, (also note that therefore it is irrelevant which one is used in stating Theorem 6). Therefore there exists a positive ϵ such that $s^+(t) > s^-(t)$ for $t \in [t_0, t_0 + \epsilon]$. However, according to Lemma 4 $s^-(t)$ can never catch up with $s^+(t)$ as long as $s_t^-(t) > 0$. Therefore $s^+(t) > s^-(t)$ for all $t > t_0$. Moreover, as noted before, $[\bar{p}_c] = -[\tau s_t]$ since $[h^{-1}] = 0$. But since $s^+ > s^-$ implies $[\tau s_t] < 0$, it follows that $[\bar{p}_c] > 0$ for all $t > t_0$.

□

4.3 Pure h-heterogeneities

Whereas in the previous section we made the restriction $[h] = 0$, we will now recreate similar results for the case $[\tau] = 0$. However, as we will see in the proof of Lemma 6 we will need an additional restriction, namely, log-convexity of $J(s)$, to make any meaningful statements about the relation between $s^+(t)$ and its equilibrium counterpart $s_e^+(t)$. Note that, as before, $s_e^+(t)$ is defined by $\frac{J(s_e^+(t))}{h^+} = \max\left(\frac{J(s^-(t))}{h^-}, \frac{J(1)}{h^+}\right)$. However, since $[h] \neq 0$ this is not reduced to a simple form like $s_e^+(t) = s^-(t)$, in contrast to the previous subsection.

Lemma 6.
Suppose Conjecture 1 holds. Furthermore, suppose $h^- > h^+$, $\tau^+ = \tau^-$, $s^+, s^- < 1$, that either s_t^- or s_t^+ are unequal to zero, and suppose $J(s)$ is log-convex. Then whenever $s^+ = s_e^+$ it holds that $s_t^+ = s_t^-$, and that $|s_{e,t}^+| > |s_t^+|$. Moreover, $s_t^- \left(\frac{\partial}{\partial t}[\tau s_t]\right) > 0$.

Proof. Since $s^+, s^- < 1$, it follows that $[p_c] = 0$. Moreover, suppose $s^+ = s_e^+$, then it holds that $\frac{J(s^+(t))}{h^+} = \frac{J(s^-(t))}{h^-}$. Therefore $[\tau s_t] = 0$, hence $s_t^+ = s_t^-$. Now, let us compute $s_{e,t}^+$ by differentiating both sides of the equation $\frac{J(s_e^+)}{h^+} = \frac{J(s^-)}{h^-}$:

$$\begin{aligned} \frac{\partial}{\partial t}\frac{J(s_e^+)}{h^+} &= \frac{\partial}{\partial t}\frac{J(s^-)}{h^-} \\ s_{e,t}^+ &= \frac{J'(s^-)J(s_e^+)}{J'(s_e^+)J(s^-)} s_t^- \end{aligned} \tag{30}$$

Where in the last line the definition of s_e^+ was used to substitute the fraction $\frac{h^+}{h^-}$. Note that exactly óne of the terms $\frac{J(s_e^+)}{J(s^-)}$ and $\frac{J'(s^-)}{J'(s_e^+)}$ is smaller then 1, and therefore we need more information about $J(s)$ in order to complete our proof. This is where the log-convexity of J comes in, which means that $\frac{\partial}{\partial s}\left(\ln J(s)\right) = \frac{J'(s)}{J(s)} < 0$ is an increasing function of s. Since $h^- > h^+$, it holds that $s_e^+ > s^-$, and therefore equation (30) infers that $|s_{e,t}^+| > |s_t^-|$. Since $s_t^- = s_t^+$, our second result follows.

Finally, again using both the definition of s_e^+ and the log-convexity of J:

$$\begin{aligned} \frac{\partial}{\partial t}[\tau s_t]\Big|_{s^+=s_e^+} &= \frac{\partial}{\partial t}\left(\frac{J(s^+)}{h^+} - \frac{J(s^-)}{h^-}\right)\Big|_{s^+=s_e^+} \\ &= \left(\frac{J'(s^+)}{h^+} - \frac{J'(s^-)}{h^-}\right) s_t^-\Big|_{s^+=s_e^+} \\ &= \left(\frac{J'(s_e^+)}{J(s_e^+)}\frac{J(s^-)}{J'(s^-)} - 1\right)\frac{J'(s^-)}{h^-} s_t^- \end{aligned} \tag{31}$$

Since the first two terms of the right side of equation (31) are negative, our last result follows. □

Lemma 6 is broadly similar to Lemma 4. Again, note the metaphor with 'catching up' - $s_e^+(t)$ can only catch up with $s^+(t)$ instead of the other way around, and when doing so the sign of $[\tau s_t](t)$ inevitably changes.

However, the similaries of Lemma 6 do not extend far. Namely, in the case with $[h] = 0$ continuity of the capillary pressure is guaranteed whenever $s^+ = s_e^+$ or $s^- = s_e^-$. When $[h] \neq 0$ however, it is possible for s^+ to have an interval of equilibrium states (for example, when $[p_c] < 0$), or to have the equilibrium state $s_e^+ = 1$ and $\frac{J(1)}{h^+} > \frac{J(s^-)}{h^-}$. In both cases $[p_c] \neq 0$ when $s^+ = s_e^+$, and therefore the reasoning in the proof of Lemma 6 does not apply. Still, it does make meaningful

predictions in the case with s^+ and s^- both unequal to 1. Now, let us consider the $[\tau] = 0$ variants of Lemma 5 and Theorem 6.

Lemma 7.
Suppose Conjecture 1 holds, and that $s_t^- = s_t^+ = 0$, $s_e^+ = s^+ < 1$, $J(s)$ *log-convex,* $\tau^+ = \tau^-$, *and* $h^- > h^+$. *Then if either* $\frac{\partial^2 s^-}{\partial t^2}$ *or* $\frac{\partial^2 s^+}{\partial t^2}$ *are unequal to zero, it holds that* $\frac{\partial^2 s^+}{\partial t^2} = \frac{\partial^2 s^-}{\partial t^2}$, $|\frac{\partial^2 s_e^+}{\partial t^2}| > |\frac{\partial^2 s^+}{\partial t^2}|$. *Moreover,* $\frac{\partial}{\partial t}[\tau s_t] = 0$, *and* $\frac{\partial^2 s^-}{\partial t^2}\left(\frac{\partial^2}{\partial t^2}[\tau s_t]\right) > 0$.

Proof. In the same line of reasoning as before, let us first compute $\frac{\partial}{\partial t} s_{e,t}^+$. Note that s_t^-, s_t^+, and $s_{e,t}^+$ are all equal to 0.

$$\begin{aligned}
\frac{\partial^2}{\partial t^2}\frac{J(s_e^+)}{h^+} &= \frac{\partial^2}{\partial t^2}\frac{J(s^-)}{h^-} \\
\frac{J''(s_e^+)}{h^+}s_{e,t}^+ + \frac{J'(s_e^+)}{h^+}\frac{\partial}{\partial t}s_{e,t}^+ &= \frac{J''(s^-)}{h^-}s_t^- + \frac{J'(s^-)}{h^-}\frac{\partial}{\partial t}s_t^- \\
\frac{\partial}{\partial t}s_{e,t}^+ &= \frac{J'(s^-)J(s_e^+)}{J'(s_e^+)J(s^-)}\frac{\partial}{\partial t}s_t^-
\end{aligned} \tag{32}$$

Moreover, since $s_t^- = 0$, equation (31) implies that $\frac{\partial}{\partial t}[\tau s_t] = 0$, and therefore $\frac{\partial}{\partial t}s_t^- = \frac{\partial}{\partial t}s_t^+$. It is now clear that $|\frac{\partial^2 s_e^+}{\partial t^2}| > |\frac{\partial^2 s^+}{\partial t^2}|$.

Finally,

$$\begin{aligned}
\frac{\partial^2}{\partial t^2}[\tau s_t]\Big|_{s^+=s_e^+} &= \frac{\partial^2}{\partial t^2}\left(\frac{J(s^+)}{h^+} - \frac{J(s^-)}{h^-}\right)\Big|_{s^+=s_e^+} \\
&= \left(\frac{J''(s^+)}{h^+} - \frac{J''(s^-)}{h^-}\right)s_t^-\Big|_{s^+=s_e^+} + \left(\frac{J'(s^+)}{h^+} - \frac{J'(s^-)}{h^-}\right)\frac{\partial}{\partial t}s_t^-\Big|_{s^+=s_e^+} \\
&= \left(\frac{J'(s_e^+)}{J(s_e^+)}\frac{J(s^-)}{J'(s^-)} - 1\right)\frac{J'(s^-)}{h^-}\frac{\partial}{\partial t}s_t^-
\end{aligned} \tag{33}$$

As before, the first two terms of the right side of equation (33) are negative, and our last result follows. □

Remark 2.
Note that in case $J(s)$ *was log-concave, similar results as the ones above could be constructed, but with flipped signs, resulting in different behavior since* $\frac{J(s_e^+)}{h^+} = \frac{J(s^-)}{h^-}$ *would still hold. In this case* s^+ *would move faster then its equilibrium state* s_e^+, *and since* $s_e^+ > s^-$ *when* $h^- > h^+$, *this would mean that* s^+ *would possibly hit the wall* $s^+ = 1$ *even when* $s_e^+ < 1$, *which is impossible when* J *is log-convex.*
The reason however that we assumed that J *was log-convex, is that log-concavity on the interval* $[0, 1]$ *is impossible whenever* $J(0) = \infty$, *as it is in our case. However, when* $J(0) < \infty$, *there would be possible discontinuities in capillary pressure when* $s = 0$.
Ironically, this means that the simple relation between states and their equilibrium as described above is only possible when there are discontinuities in pressure around $s = 1$ *or* $s = 0$.
Finally, note that alternative models for $J(s)$, *like the version from van Genuchten [2], is neither log-concave or log-convex.*

Theorem 7.
Suppose $h^- > h^+$, $s_t^-(t_0) = s_t^+(t_0) = 0$, $s^+(0), s^-(0) < 1$ *and* $\frac{J(s^+(t_0))}{h^+} = \frac{J(s^-(t_0))}{h^-}$.
Then if $\frac{\partial s_t^-(t)}{\partial t}|_{t=t_0} > 0$, *and* $s_t^-(t) > 0$, $s^-(t), s^+(t) < 1$, *for all* $t > t_0$, *it holds that* $s_e^+(t) > s^+(t)$ *and* $[\tau s_t] > 0$ *for all* $t > t_0$.

Similarly, if $\frac{\partial s_t^-(t)}{\partial t}|_{t=t_0} < 0$, $s^+(0) < 1$ *and* $s_t^-(t) < 0$, $s^-(t), s^+(t) < 1$, *for all* $t > t_0$, *it holds that* $s_e^+(t) < s^+(t)$ *and* $[\tau s_t] < 0$ *for all* $t > t_0$.

Proof. Let us consider the case $\frac{\partial s_t^-(t)}{\partial t}|_{t=t_0} > 0$. Then Lemma 7 states $\frac{\partial s_{e,t}^+(t)}{\partial t}|_{t=t_0} > \frac{\partial s_t^+(t)}{\partial t}|_{t=t_0} > 0$. Therefore $s_e^+(t) > s^+(t)$ for all $t \in [t_0, t_0 + \epsilon]$ for a certain positive ϵ. But Lemma 6 states that $s^+(t)$ can never catch up with $s_e^+(t)$ as long as $s_t^-(t) > 0$. Therefore $s_e^+(t) > s^+(t)$ for all $t > t_0$ and our results follow.

The case for $\frac{\partial s_t^-(t)}{\partial t}|_{t=t_0} < 0$ is similar. □

Note that this time around we can not make a prediction about $[\bar{p}_c]$ in both cases. For example, when $[\tau s_t] < 0$ it follows that $[\bar{p}_c] > 0$, but when $[\tau s_t] > 0$ it is not guaranteed that $[\bar{p}_c] < 0$.

Moreover, Lemma 6 and Theorem 7 presuppose that the capillary pressure p_c is continuous. When $[p_c] \neq 0$ key results can easily be extended on a case by case basis, but care must be taken when $[h] \neq 0$. For example, starting up from a equilibrium position with $[h] = 0$ means starting from a position with $[p_c] = 0$, since the only equilibrium states are $s^+ = s^-$, and the results from Theorem 6 extend over the case with $[p_c] \neq 0$, but with the strict inequality concerning equilibrium states being replaced with non-strict versions. However, when $[\tau] = 0, [h] \neq 0$, it is possible to start from an equilibrium state with discontinuous capillary pressure. This can lead to a switch in behaviour, where it is first determined by the discontinuity $[p_c] \neq 0$, and afterwards by the sign of s_t^-, conform Theorem 7.

Finally, the case of a a smooth and strictly decreasing $s^-(t)$ starting from a equilibrium state with discontinuous capillary pressure is also one of the few in which $s_e^+(t)$ 'catches up' with $s^+(t)$ (remember that the other way around is not allowed for non-zero s_t^-, according to Lemma 6). This scenario has deep implications when incorporating the flux condition, as will be seen in Chapter 5. First, for an example of all the different scenarios, consider the numerical results in the next section.

4.4 Simulation pressure condition at interface

As mentioned before, we will use some of the same numerical conventions as used in [3]. So:

$$\begin{aligned} J(s) &= s^{-1/2} \\ k_{rw}(s) &= s^2 \\ k_{rn}(s) &= (1-s)^2 \\ N_c &= 1 \\ M &= 1 \\ \phi^- &= 1 \\ \phi^+ &= 1 \end{aligned}$$

Whereas the remaining variables, $h^{\pm} = \sqrt{\frac{\phi^{\pm}}{k^{\pm}}}$ and $\tau^{\pm}$, will vary. For $s^-(t)$ we will use both a decreasing and increasing logistic function, specifically, $s^-(t) = \frac{a}{1+e^t}$ or $s^-(t) = \frac{a}{1+e^{-t}}$, with a equal to either 1 or $\frac{1}{2}$. To calculate $s^+(t)$ we will use the form of the pressure condition mention in Section 4.1, i.e. we will use formula (25):

$$\begin{aligned} s_t^+ &= G_1(s^+,t) && \text{if} \quad s^+ < 1 \vee G_1(s^+,t) \leq 0 \\ &= G_2(s^+,t) && \text{if} \quad s^+ = 1 \wedge G_1(s^+,t) > 0 \end{aligned} \tag{34}$$

Finally, we will put the interface at $x = 0$.

Simulation pure h-heterogeneities

Below you will see the calculated $s^+(t)$, for both the increasing and decreasing logistic functions, and with τ taking on the values $\{5, 1, 0.2\}$, with $a = 1$ for Figures 4 and 5, and $a = 1/2$ for Figure 6. In Figures 4 and 6 we will let $h^- = 2$ and $h^+ = 1$, whereas in Figure 5 those two are reversed. Moreover, the corresponding equilibrium state $s_e^+(t)$ will also be plotted.

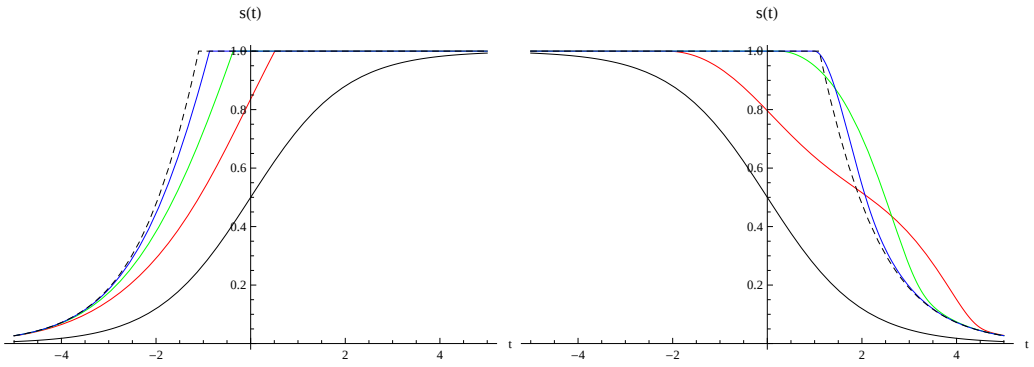

Figure 4: $s^-(t)$ *(Black)*, $s_e^+(t)$ *(Black, Dashed)*, and $s^+(t)$ for various $\tau^- = \tau^+$ *(Colored)*, with $h^- > h^+$

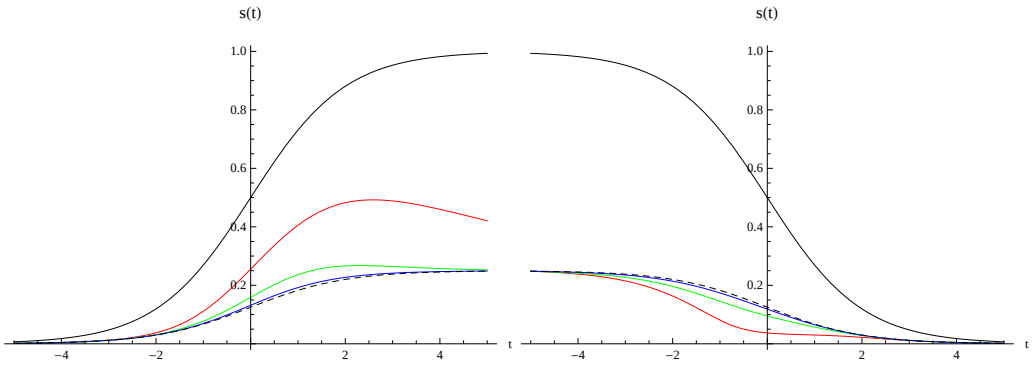

Figure 5: $s^-(t)$ *(Black)*, $s_e^+(t)$ *(Black, Dashed)*, and $s^+(t)$ for various $\tau^- = \tau^+$ *(Colored)*, with $h^+ > h^-$

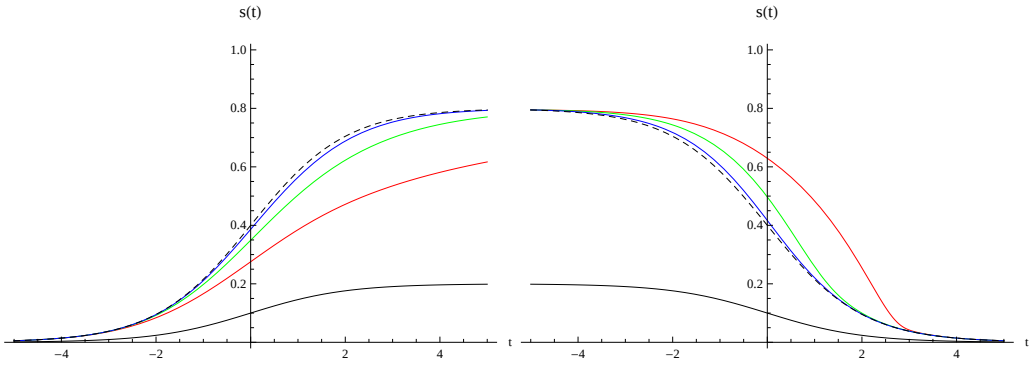

Figure 6: $s^-(t)$ *(Black)*, $s_e^+(t)$ *(Black, Dashed)*, and $s^+(t)$ for various $\tau^- = \tau^+$ *(Colored)*, with $h^- > h^+$ and $s^-(\pm\infty) < 1$

Simulation pure τ-heterogeneities

Again, both the increasing and decreasing logistic functions will be used for $s^-(t)$, with $a = 1$. We will take $h^+ = h^- = 1$, and for Figure 7 we use $\tau^+ = 2\tau^- = \{10, 2, 0.4\}$, whereas in Figure 8 this will be reversed.

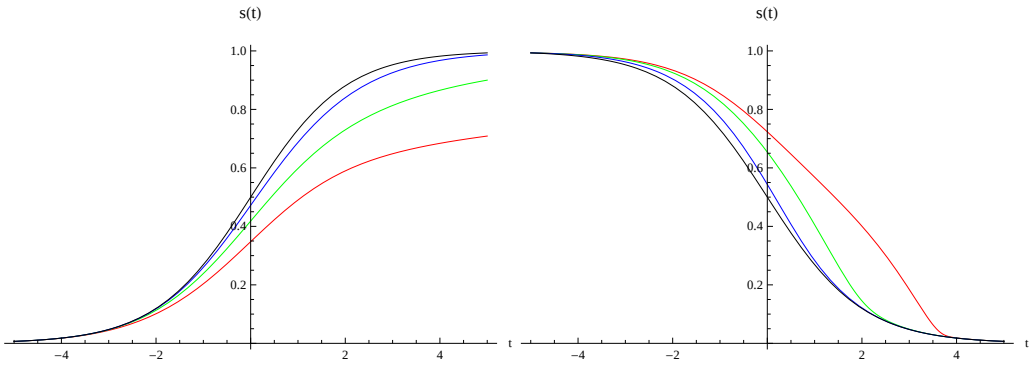

Figure 7: $s^-(t)$ *(Black)*, and $s^+(t)$ for various $2\tau^- = \tau^+$ *(Colored)*

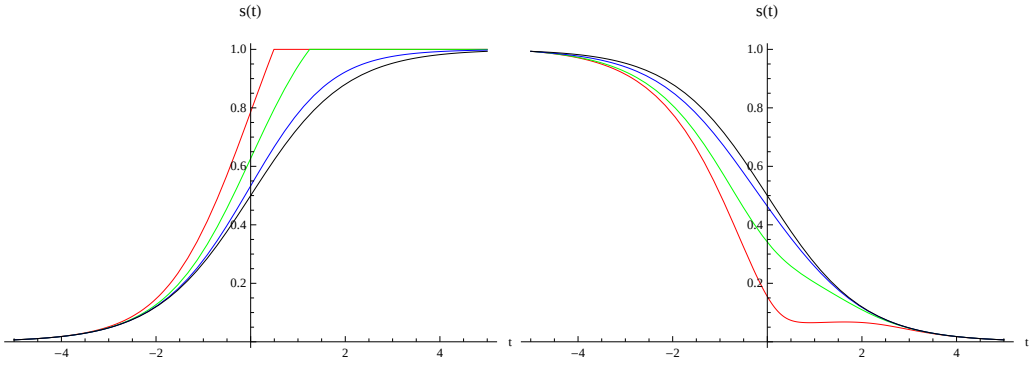

Figure 8: $s^-(t)$ *(Black)*, and $s^+(t)$ for various $2\tau^- = 2\tau^+$ *(Colored)*

Discussion

First note that as $\tau \to 0$, the non-equilibrium $s^+(t)$ moves closer and closer to its equilibrium counterpart, $s_e^+(t)$, as expected. Secondly, note how the shapes of the wavefronts of s^- asymmetrically effects s^+, as expected, clearly demonstrating the difference between inflow and outflow-processes and showing the case for $\tau > 0$ is an irreversible processes, in contrast with $\tau = 0$.

Moreover, we can see that the relationships between $s^+(t)$ and $s^-(t)$, and between $s^+(t)$ and $s_e^+(t)$, behave as we predicted in Sections 4.3 and 4.4, including the temporary breakdown in ordering of $s^+(t)$ and $s_e^+(t)$ for a decreasing wavefront with $h^- > h^+$, as shown Figure 4 and which was mentioned in the end of section 4.3.

Finally, note that while $s^+(t)$ has not 'catched up' with $s_e^+(t)$ in Figure 5, this distance seems to be decreasing more rapidly, until it catches up, overshoots, and eventually and smoothly goes to zero. This means that not only $[\tau s_t]_t < 0$ when $[\tau s_t] = 0$ as proven in Lemma 4, but $[\tau s_t]_t < 0$ while $[\tau s_t] \geq 0$ (and as it seems also $[\tau s_t]_{t,t} < 0$. We could not rigourously prove this, even for strictly decreasing $s^-(t)$ and $s^+(t)$. A possible avenue would be to prove that zeros of $[\tau s_t]_t$ and $[\tau s_t]_{t,t}$ do not occur while $[\tau s_t] > 0$ (and possible other restrictions), and noting that $[\tau s_t]_t < 0$ is zero at the time the pressure becomes continuous (since then $s_t^- < s_t^+ = 0$, and adaptations of Lemma 6 and 7 can be used). Yet, alas without proof, this result has as noted still deep implications for the next chapter.

5 Simulation dynamic flow around the interface

In the previous section we used the extended pressure condition to model the saturations at both sides of the interface. In case one of the two was given we could uniquely determine the other, and achieved some insight in the effect of non-equilibrium interface conditions. But to fully understand this phenomenon we will also have to use the flux interface condition, and model the saturation around the interface. In this section, we intend to do just that.

General analytical results are however beyond the scope of this report. That is why we will focus on numerical simulations and simple analytical examples. First we will introduce an explicit and linear difference scheme, and will study both the numerical stability of the simulation, and the behaviour of the saturation at and around the interface.

Although the simulation was run for a wide range of variables and initial distributions, for the sake of clarity we will restrict ourselves to two examples, which will be run for several values of τ. Both involve the interaction of a stream of oil with the interface, with the less coarse medium being fully saturated ($s(x,0) = 1$), and both have a initial discontinuous capillary pressure at $x = 0$. The first is a hypothetical example with $s(x,0)$ also constant on the left side of the interface, to both study the results in a simplified form and providing an analytical starting point to explain them. The second example is a more general version of an oil-water front, similar to the one studied in [**3**]. Moreover, our functional dependencies and variables will be the same as those in [**3**].

Although in our numerical analysis we will both simulate and study the behaviour of dynamic flow at an entire interval around the interface, it is important to note that the focus of this research is still primarily concerned with the behaviour át or near the interface. For general results about dynamic flow, such as the existence of traveling waves, one should consult for example [**2**]. Interestingly enough, it appears that this restriction opens up the way for seemingly universal behaviour over a wide range of initial saturations, as will be seen in the rest of this chapter.

5.1 Numerical Scheme

We will approximate the differential equations in successive discrete steps, by solving a corresponding linear system, and divide the interval $[x_l, x_r]$ into a grid. The boundary conditions on the discontinuous material interface will be modeled by splitting the coordinate of the interface in two different points, and imposing a relation between the saturation on these points.

To be specific, the interval will be split divided into two groups of N points all Δx apart, namely $x_{-N}, \ldots, x_{0-}$ and $x_{0+}, \ldots, x_N$, where $x_{-N} = x_l$, $x_N = x_r$, and with the interface on $x = 0$. The saturation on a point x_k at time n (with n discrete) will be denoted by u_k^n, with the pressure denoted similarly as p_k^n. The saturations at the points x_l and x_l are fixed, such that $u_{-N}^n = u_l$, and $u_N^n = u_r$ for all n.

Remember that, with u the saturation, it holds that

$$\phi \frac{\partial u}{\partial t} + q \frac{\partial f_w}{\partial x} + \frac{\partial}{\partial x}\left(k\bar{\lambda}(s) \frac{\partial p_c}{\partial x} \right) = 0 \tag{35}$$

In equation (35) we will replace the partial derivatives with their discrete approximations, with timestep Δt. But first, let us define $f(s) := q * f_w(s)$, $H_l(s) := k_l\bar{\lambda}(s)$, $H_r(s) := k_r\bar{\lambda}(s)$. Furthermore, suppose $q > 0$, and using the so-called upwind approximation for the derivative of the flow function, we get for $k \neq -N, N$:

$$\left.\frac{\partial u}{\partial t}\right|_{u=u_k^n} \approx \frac{u_k^{n+1} - u_k^n}{\Delta t} \tag{36}$$

$$\left.\frac{\partial f}{\partial x}\right|_{u=u_k^n} \approx \frac{f(u_k^n) - f(u_{k-1}^n)}{\Delta t} \tag{37}$$

$$\left.\frac{\partial (H\partial p)}{\partial x^2}\right|_{u=u_k^n} \approx \frac{1}{\Delta x}\left(H_{k+\frac{1}{2}}^n \frac{p_{k+1}^n - p_k^n}{\Delta x} - H_{k-\frac{1}{2}}^n \frac{p_k^n - p_{k-1}^n}{\Delta x} \right) \tag{38}$$

$$\tag{39}$$

Where the appropriate indices l,r hold for the functions H and p on the left and right side of the interface, and $H_{k-\frac{1}{2}}^n = H\left(\frac{u_k^n + u_{k-1}^n}{2}\right)$.

Now, when $k \neq -K, K, 0^+, 0^-$, we can substitute (35) as follows:

$$\begin{aligned} \phi \frac{u_k^{n+1} - u_k^n}{\Delta t} \quad + \quad & \frac{f(u_k^n) - f(u_{k-1}^n)}{\Delta x} + \frac{1}{\Delta x}\left(H_{k+1/2}^n \frac{p_{k+1}^n - p_k^n}{\Delta x} - H_{k-1/2}^n \frac{p_k^n - p_{k-1}^n}{\Delta x} \right) = 0 \\ p_k^n \quad = \quad & \frac{J(u_k^n)}{h} - \tau \frac{u_k^{n+1} - u_k^n}{\Delta t} \end{aligned}$$

Note that at time n in the equations this system in linear in the unknown variables u_k^{n+1} and p_k^n (for all $k \neq -N, N$). Now suppose p_c is continuous over the interface. Then adding both the flux and extended pressure condition to the system above, and arranging the equations such that all the unknown variables are on one side, we get

$$
\begin{aligned}
p^n_k &+ \tau\frac{u^{n+1}_k}{\Delta t} = \frac{J(u^n_k)}{h} + \tau\frac{u^n_k}{\Delta t} \qquad k \neq -N, N \\
p^n_{0+} &= p^n_{0-} \\
\phi\frac{u^{n+1}_{-N+1}}{\Delta t} &+ \frac{1}{(\Delta x)^2}\left(-(H^n_{-N+1/2} + H^n_{-N+3/2})p^n_{-N+1} + H^n_{-N+3/2}(p^n_{-N+2})\right) \\
&= \phi\frac{u^n_{-N+1}}{\Delta t} + \frac{f(u^n_{-N}) - f(u^n_{-N+1})}{\Delta x} - \frac{1}{(\Delta x)^2}H^n_{-N+1/2}p_l \\
\phi\frac{u^{n+1}_k}{\Delta t} &+ \frac{1}{(\Delta x)^2}\left(H^n_{k+1/2}p^n_{k+1} - (H^n_{k+1/2} + H^n_{k-1/2})p^n_k + H^n_{k-1/2}(p^n_{k-1})\right) \\
&= \phi\frac{u^n_k}{\Delta t} + \frac{f(u^n_{k-1}) - f(u^n_k)}{\Delta x} \qquad k \neq -N, -N+1, 0^-, 0^+, N-1, N \\
\phi\frac{u^{n+1}_{N-1}}{\Delta t} &+ \frac{1}{(\Delta x)^2}\left(-(H^n_{N-1/2} + H^n_{N-3/2})p^n_{N-1} + H^n_{N-3/2}(p^n_{N-2})\right) \\
&= \phi\frac{u^n_{N-1}}{\Delta t} + \frac{f(u^n_{N-2}) - f(u^n_{N-1})}{\Delta x} - \frac{1}{(\Delta x)^2}H^n_{N-1/2}p_r \\
H^n_{-1/2}\frac{p^n_{0-} - p^n_{-1}}{\Delta x} &- H^n_{1/2}\frac{p^n_1 - p^n_{0+}}{\Delta x} = f(u_{0+}) - f(u_{-1})
\end{aligned}
$$

Where the functions H and p are dependent on the side of the interface. Note that in total these are $(2N-2)+1+(2N-4)+1 = 4N-4$ equations over $4N-4$ unknowns, so that it can be reframed as the linear system $\mathbf{Q_n} \cdot \mathbf{v_{n+1}} = \mathbf{l_n}$, where v_n is the vector $(u^{n+1}_{-N+1}, \ldots, u^{n+1}_{N-1}, p^n_{-N+1}, \ldots, p^n_{N-1})$ of length $4N-4$, and the square matrix Q_n and the vector l_n are only dependent on v_n.

However, whenever $u^n_{0-} = 1$ and/or $u^n_{0+} = 1$, the linear system changes. First of all, $p_{0-} = p_{0+}$ does possibly not hold. Second, note if $u^n_{-1}, u^n_{0-}, u^n_{0+}, u^n_1$ are áll equal to 1, the flux condition reduces to $0 = 0$. In both cases, the linear system becomes indetermined. This can be resolved by checking continuity of pressure after every iteration and involving the complete extended pressure condition.
Namely, if either u^n_{0-} or u^n_{0+} overshoots 1 they will be reset to 1, and pressures will be compared, resulting in the state of the program to be either set to DISCONTINUOUS-RIGHT, DISCONTINUOUS-LEFT, or CONTINUOUS. If for example, after this correction, $p^n_{0-} \leq \frac{J(u^n_{0+})}{h^+}$ and $u^n_{0+} = 1$, for the next iteration the condition $p^n_{0+} = p^n_0$ will be replaced with $u^{n+1}_{0+} = 1$, leading to a new and non-singular equation $\mathbf{Q_n} \cdot \mathbf{v_{n+1}} = \mathbf{l_n}$. The case for $u^n_{0-} = 1$ is similar. Moreover, if after an iteration starting from a state DISCONTINUOUS-RIGHT lets u^n_{0+} overshoot into $u^n_{0+} < 1$, the state will be reset to CONTINUOUS.

Finally, the problem with $\{u^n_{-1}, u^n_{0-}, u^n_{0+}, u^n_1\} = 1$ will be resolved by dropping the flux and pressure conditions, and setting $u^{n+1}_{0-} = 1, u^{n+1}_{0+} = 1$.

Note however, that our numerical scheme does not work with very small values of u, since $J(u) \to \infty$ as $u \to 0$. Replacement of identities in Q could me made to ensure correctness, but it would still lead to stability around these points. Therefore, we will only use values of u above a certain threshold.

Conventions

As noted before, in our numerical simulations we use certain instances of the k_{rn}, k_{rw}, $J(s)$ and numerical variables. Namely, the same conventions as used in [3]:

$$\begin{aligned} J(s) &= s^{-1/2} \\ k_{rw}(s) &= s^2 \\ k_{rn}(s) &= (1-s)^2 \\ k^- &= 1 \\ k^+ &= 0.1 \\ N_c &= 1 \\ M &= 1 \\ \phi &= 1 \end{aligned}$$

Moreover, except for some of the examples to illustrate stability issues, both the Horizontal Front and the Oil-Water Front have the following numerical parameters:

$$\begin{aligned} x_r &= 1 \\ x_l &= -1 \\ u_r &= 1 \\ \Delta x &= 0.005 \\ N &= 200 \\ \Delta t &= 10^{-4} \\ \tau &= \{0.2,\ 0.1,\ 0.05,\ 0.025,\ 0.0125,\ 0.00625\} \end{aligned}$$

5.2 Observations & Discussion

5.2.1 Stability

Because of the scope of this article we will not place explicit bounds of the error inherent to the numerical scheme. As a rule of thumb we used small enough Δt and Δx such that a simulation ran with half of those parameters did not differ much from the original simulation. However we will show two important considerations in choosing Δt, Δx and τ.

Free boundaries

Consider Figures 9 and 11, where we show the comparison between the speed of the free boundary for a certain initial saturation, and lines with a slope of $\frac{\Delta t}{\Delta x}$.

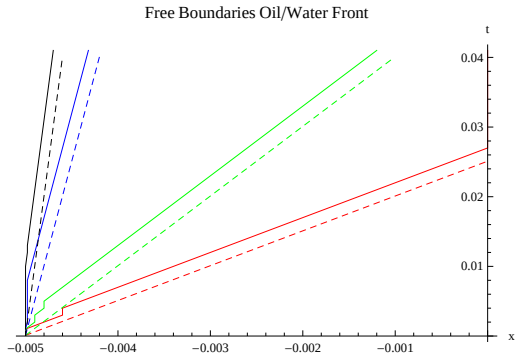

Figure 9: Free Boundary Plot for $\Delta t = 10^{-3}$, $K = \{50, 100, 500, 1000\}$, {Red, Green, Blue, Black}

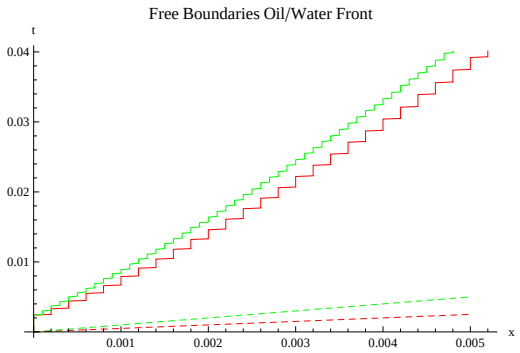

Figure 10: Boundary Plot for $\Delta t = 10^{-4}$, $K = \{50, 100\}$, {Red, Green }

It is easy to see that the speed of the free boundary in our simulation v_{sim} is always smaller than $v_{num} = \frac{\Delta x}{\Delta t}$. This is because of the way our program handles free boundaries. If u^n_{k-1}, u^n_k and u^n_{k+1} are equal to 1 for certain k, n, it holds that $u^{n+1}_k = 1$. This means that the free boundary between oil and water can only move one gridpoint per timestep, i.e. $v_{sim} \leq v_{num}$. Thus, for an accurate numerical representation of free boundaries, let alone the flow, it should be that the actual speed of the free boundary v should be much smaller than $v_{num} = \frac{\Delta x}{\Delta t}$.

Oscillation at the interface

Consider Figure 11, in which s^- is plotted against t for a certain initial saturation with $\tau = 0.01$. For clarity, the various points were not joined. It is clear that as time progresses, a certain type of resonance occurs as the simulation becomes increasingly unstable (for the interested readers, one can even discern period doubling). This happens only for very small values of τ, but this error is very easy to spot. That is why for our simulations we used $\tau > 0.001$.

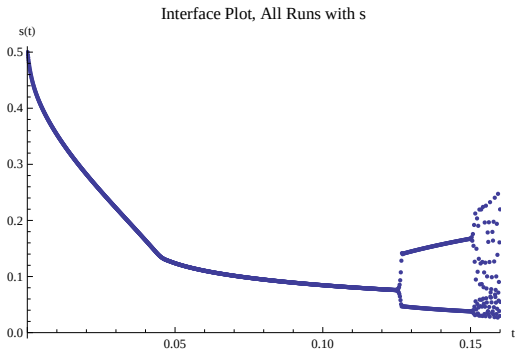

Figure 11: Interface Plot for s^-, for $\tau = 0.001$

5.2.2 Horizontal Front

As noted, the initial saturation is piecewise constant. To be precise,

$$s(x,0) = \begin{cases} a, & \text{if} \quad x < 0, \\ 1, & \text{if} \quad x > 0. \end{cases} \tag{40}$$

Note that this initial saturation would not be possible when $\tau = 0$ since it would violate the flux condition over the interface. However, for non-zero τ this is not a problem and in this case there exists an unique $s(x,t)$ for every value of a.

As for the values of the numerical parameters we have

$$\begin{aligned} a &= 0.4 \\ x_r &= 1 \\ x_l &= -1 \\ u_l &= a \\ u_r &= 1 \\ \Delta x &= 0.005 \\ N &= 200 \\ \Delta t &= 10^{-4} \\ \tau &= \{0.2,\ 0.1,\ 0.05,\ 0.025,\ 0.0125,\ 0.00625\}. \end{aligned}$$

Before we dive into a detailed analysis, let us first consider the global behaviour of both the saturation and the capillary pressure. See Figure 12 for $s(x,t)$ and $p_c(x,t)$ at various t. Note that, for sake of clarity, we zoomed in to the interval of $[-0.15, 0.15]$. At first glance it appears that while those with higher τ have a slower initial change in saturation yet have a higher capillary pressure. Moreover these orderings invert a couple of times both before and after breaking the pressure discontinuity at $x = 0$, and the capillary pressures p_c^- even briefly converge right before reaching continuity with p_c^+.

Note that the boundary conditions are actually split in two phases, one with a discontinuous pressure and with a continuous pressure over the interface. For every τ there is a breaking point at time t_b, such that for the corresponding simulation it holds that:

$$\begin{aligned} F(0,t) = 1,\ [p_c(t)] > 0 \quad &\text{if} \quad t < t_b, \\ [p_c(t)] = 0 \quad &\text{if} \quad t \geq t_b. \end{aligned} \tag{41}$$

Before $t < t_b$ there is no pressure continuity, and thus the flow is completely independent from the parameters of the medium on the right side of the interface. Therefore the convergence of capillary pressure p_c^- right before the breaking point must be pure coincidence, since the breaking point is dependent on h^+. To avoid such dubious observations one could study the first phase separately (the second phase is however dependent on the first). That is why we ran the above simulations two times, once with the original $h^+ = \sqrt{0.1}$, and once with an effective $h^+ = 0$. In this second case the breaking point never occurs, and can be used to study the first phase only.

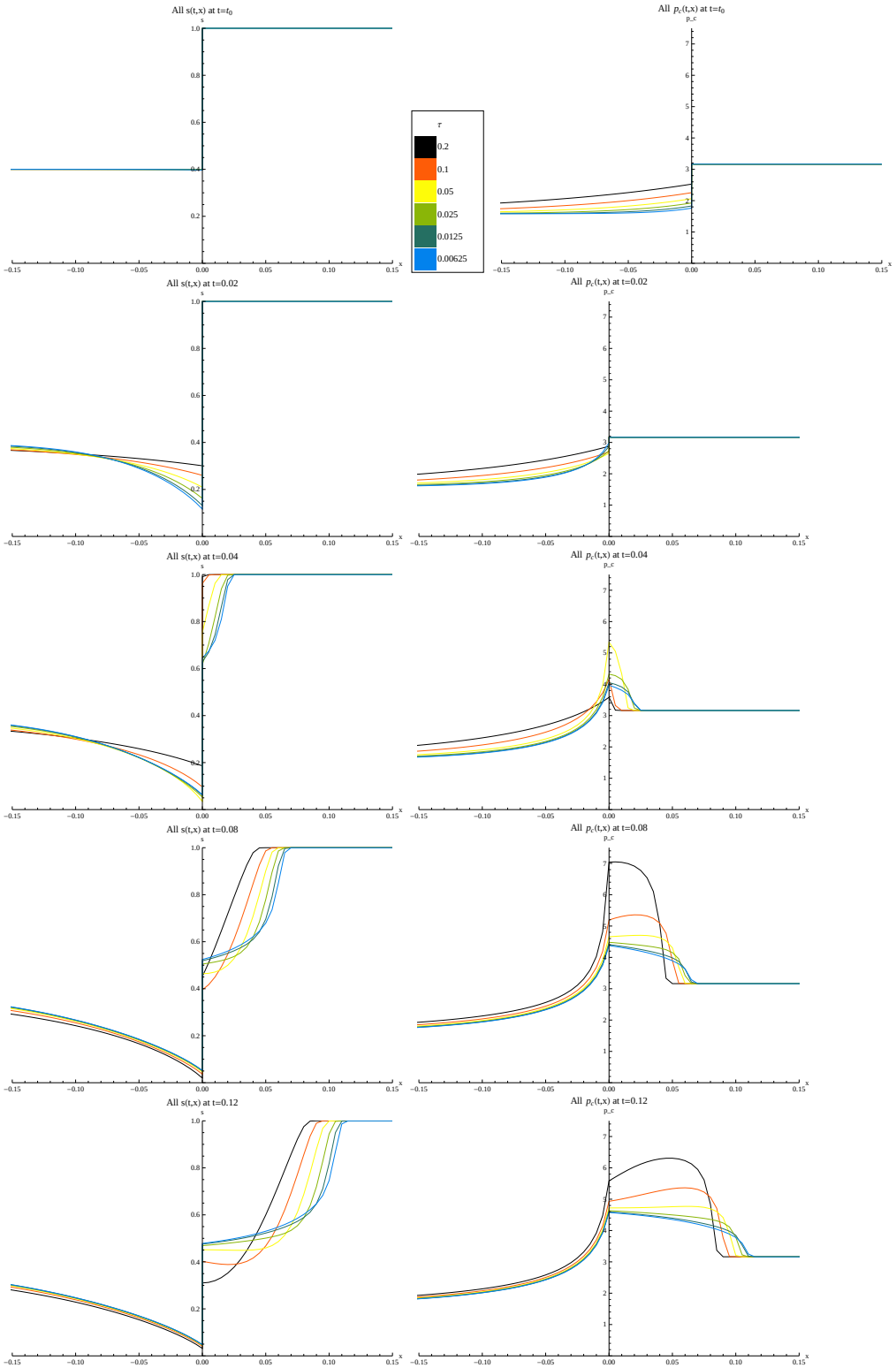

Figure 12: Plots of both $s(x,t)$ and $p_c(x,t)$ for various t

5.2.2.1 Behaviour at interface for $h^+ = 0$

See Figure 13 for the behaviour of the saturation and capillary pressure at the interface. Since a breaking point never occurs, $s^-(t)$ seems to become 0 in finite time. Now, first note that the convergence of capillary pressure would not hold for all k^+ since for a high enough breaking point they diverge again. Secondly, it appears as if there is a critical value $\tau_c \sim 0.05$ such that s_t^- briefly and roughly converges to a single value for all $\tau < \tau_c$, with $s_{t,t}^- = 0$ for $\tau = \tau_c$. Although one can not infer a non-analyticity on the basis of only six values (apart from the question if the equations would even allow a non-analyticity), the division does seem quite sharp.

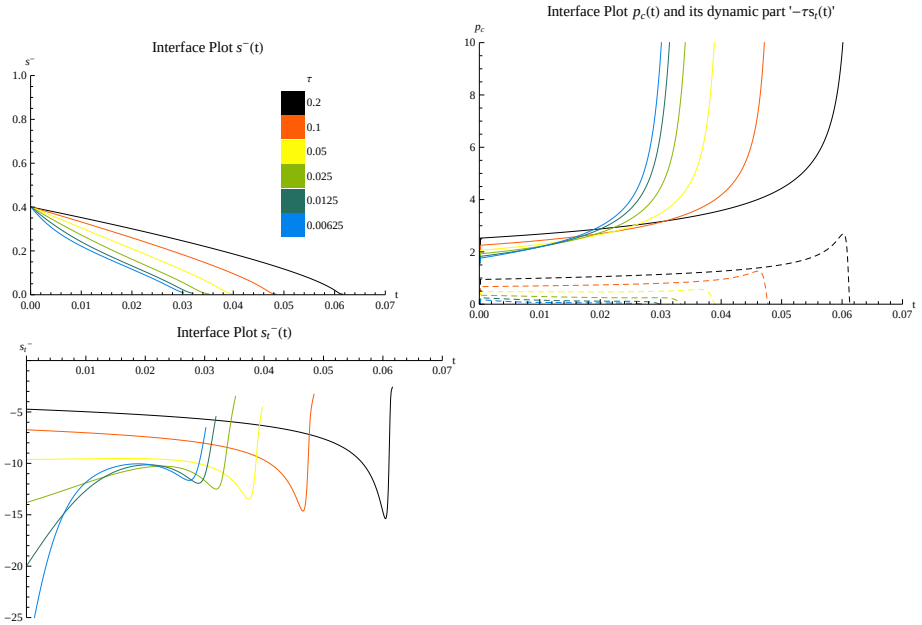

Figure 13: Interface Plots for $s^-(0,t)$, $s_t^+(0,t)$ and $p_c(0,t)$

Finally, note that the ordering in initial capillary pressure is completely due to its dynamic part $-\tau s_t^-$, as is expected since $J(s(x,0))$ is constant. However, this means that s_t^- becomes smaller for larger τ (as is seen in the Interface Plot of s_t^-), but large enough such that this ordering in τs_t^- is inverted. Not only explains this why p_c will be smaller for larger τ for large t - since s^- is bigger and therefore the static term $J(s^-)/h^-$ eventually takes over - but this also begs the question if s_t is on the order of τ^{-k}, with k between 0 and 1.

As we will see below, we can even make a stronger statement, namely that $s_t^-(0) \sim c\tau^{-1/2}$ for some constant c, see Figure 14. As is clearly seen, when scaling for $\tau^{-1/2}$ all values of $s_t^-(0)$ converge to roughly the same point. Moreover, for $\tau > \tau_c$ they even roughly coincide for $t > 0$, before eventually diverging. Inspired by this scaling behaviour we also found an (although ad-hoc) appropriate scaling for t such that for $\tau > \tau_c$ the overal shape of s_t seem to converge, and specifically the time t_e such that $s^-(t_e) = 0$. However in this case they do not coincide anymore for small t. However, it should be noted that both similarities only occur at or near the interface. For x further away from zero by even a small number as 0.05, no scaling in form of τ^k seemed to exist between the various simulations.

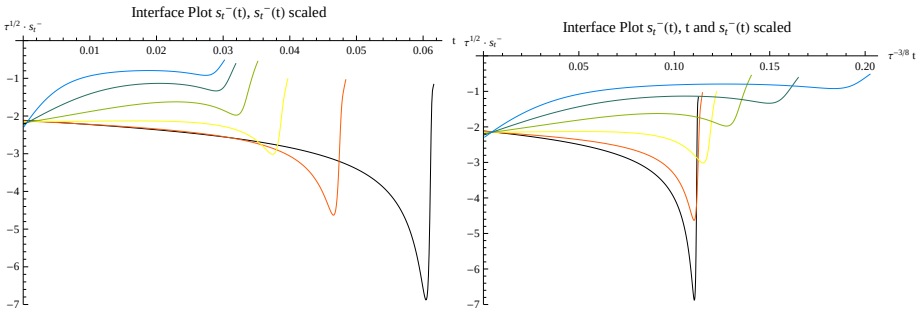

Figure 14: Interface Plots for s_t^-, scaled with $s_t^- := \tau^{1/2} s_t^-$ and $t := \tau^{-3/8} t$

5.2.2.2 Analytical analysis of scaling and criticality for $h^+ = 0$

It must be noted that these scalings are not trivial, but a hint can be found in an appropriate coordinate scaling. If both s_t and t would be scaled according to Figure 14, it would correspond roughly with the coordinate transformation $t := \frac{t}{\sqrt{\tau}}$. Now note that applying the coordinate transformation $\hat{t} := \frac{t}{\sqrt{\tau}}$ and $\hat{x} := \frac{x}{\sqrt{\tau}}$ to equation **(13)** would lead to:

$$\begin{aligned}
\frac{\partial s}{\partial \hat{t}} + \frac{\partial}{\partial x}\left(f(s) + H(s)\frac{\partial}{\partial x}\left(\frac{J(s)}{h} - \tau\frac{\partial s}{\partial t}\right)\right) &= 0 \\
\frac{\partial s}{\partial \hat{t}}\frac{1}{\sqrt{\tau}} + \frac{1}{\sqrt{\tau}}\frac{\partial}{\partial \hat{x}}\left(f(s) + H(s)\frac{1}{\sqrt{\tau}}\frac{\partial}{\partial \hat{x}}\left(\frac{J(s)}{h} - \frac{\tau}{\sqrt{\tau}}\frac{\partial s}{\partial \hat{t}}\right)\right) &= 0 \\
\frac{\partial s}{\partial \hat{t}} + \frac{\partial}{\partial \hat{x}}\left(f(s) + H(s)\frac{\partial}{\partial \hat{x}}\left(\frac{1}{\sqrt{\tau}}\frac{J(s)}{h} - \frac{\partial s}{\partial \hat{t}}\right)\right) &= 0.
\end{aligned}$$

The statement that for large τ the scaled versions of **(13)** would converge, is therefore equal to the statement that equations with the adjusted capillary pressure $p_{c,\epsilon} = \epsilon\frac{J(s)}{h} - s_t$ would converge as $\epsilon \to 0$. Whether this is actually true is not as clear cut (note that $J(s) \to \infty$ as $s \to 0$), but it does provide a plausible explanation why this scaling occurs, and why it breaks down for small τ or further away from the interface. However, it does not explain why s_t^- is exactly proportional to $\tau^{-1/2}$ for all τ in our example, and why the breakdown in scaling in t quite sharply corresponds to the same division around a certain critical τ_c as noted before.

However, because of the simple shape $s(x, 0)$, it ís possible to iteratively and analytically derive the partial derivatives of a idealized version of s with respect to t at $t = 0$ in closed form. As is clear, that is also a reason this example was chosen. Because of the complexity of this process we only provide the first two derivatives, $s_t(x, 0)$ and $s_{t,t}(x, 0)$. From these it is not possible to explain all the above observations, but it does provide some valuable insight.

Instead of the interval $[x_l, 0]$ we consider the half-open interval $(-\infty, 0]$, reducing the boundary conditions in the case for $h^+ = 0$ to

$$\begin{aligned}
s(-\infty) &= a \\
F(0, t) &= 1
\end{aligned}$$

Moreover let $H(s) = k\bar{\lambda}(s)$. Then with our functional parameters, we know from **(13)** that

$$\frac{\partial s}{\partial t} + \frac{\partial}{\partial x}\left(f(s) + H(s)\frac{\partial}{\partial x}\left(\frac{J(s)}{h} - \tau\frac{\partial s}{\partial t}\right)\right) = 0 \tag{42}$$

However, since $s(x,0)$ is constant, the equation can be greatly simplified for $t=0$.

$$\begin{aligned}\frac{\partial s}{\partial t} - H(s)\tau\frac{\partial^3 s}{\partial x^2\partial t} &+ f'(s)\frac{\partial s}{\partial x} + H'(s)\frac{\partial s}{\partial x}\cdot\frac{\partial}{\partial x}\left(\frac{J(s)}{h} - \tau\frac{\partial s}{\partial t}\right) + H(s)\frac{\partial^2}{\partial x^2}\left(\frac{J(s)}{h}\right) = 0\\ \frac{\partial s}{\partial t}|_{t=t_0} &- H(a)\tau\frac{\partial^3 s}{\partial x^2\partial t}|_{t=t_0} = 0\\ s_t(x,0) &- H(a)\tau\frac{\partial^2}{\partial x^2}s_t(x,0) = 0 \qquad (43)\end{aligned}$$

Equation **(43)** is a simple second-order differential equation in $s_t(x,0)$, with a general solution of

$$\begin{aligned}s_t(x,0) &= c_1 e^{\alpha x} + c_2 e^{-\alpha x}, \qquad \text{with } \alpha \text{ being} \qquad (44)\\ \alpha &= \frac{1}{\sqrt{H(a)\tau}} \qquad (45)\end{aligned}$$

And since $s_t(x,0) = -\frac{\partial F}{\partial x}|_{t=t_0}$ we get a general solution for the flux at $t=0$, $F(x,0)$, by integrating:

$$F(x,0) = \frac{-c_1}{\alpha}e^{\alpha x} + \frac{c_2}{\alpha}e^{-\alpha x} + c_3 \qquad (46)$$

However, since $F(0,0)=1$ and $F(-\infty)=f(a)$ it follows that $c_2=0$. Moreover,

Theorem 8. *For all x we have*

$$\begin{aligned}F(x,0) &= (1-f(a))e^{\alpha x} + f(a)\\ s_t(x,0) &= \alpha(f(a)-1)e^{\alpha x}\end{aligned}$$

For $x=0$ we therefore have the very simple expression for $s_t^-(0) = s_t(0,0)$,

$$s_t^-(0) = \frac{f(a)-1}{\sqrt{\tau H(a)}}. \qquad (47)$$

From Theorem 8 it follows why $s_t^-(0) \sim \tau^{-1/2}$, and applying the previously mentioned transformation $\hat{t} := \tau^{-1/2}t$ and $\hat{x} := \tau^{-1/2}x$ would lead to an $s_t(\hat{x},\hat{t})$ fully independent from τ. It also explains why this similarity rapidly ends for $x \neq 0$ when no coordinate transformation is used, because of the exponential term $e^{\alpha x}$. Moreover, note that the term $\alpha e^{\alpha x} \to 0$ if $x<0$ and $\tau \to 0$, and goes to infinity if $x=0$. Thus $F(x,0)=0$ for all $x<0$, with $F(0,t)=1$. Therefore, the case for $\tau=0$ can be interpreted as one with a discontinuity in the initial flux, in which a possible free boundary emerges, with a apparent continu but non-smooth $s(x,t)$ for $x<0$ as limit for $\tau \to 0$. However, the technical difficulties working with these kind of discontinuities are beyond us. Nevertheless, this example was meant as a test case for the variation in τ, and we will focus on those phenomena.

Although the above procedure can be repeated, to better understand the iteration it is best to start from a series perspective. Suppose $s(x,t)$ can be expanded in a Taylor series around $t=0$:

$$s = \sum_i^\infty \frac{P_i(x)}{i!}t^i \qquad (48)$$

Where obviously $P_0(x)=a$, $P_1(x)=s_t(x,0)$ and $P_1(x)=s_{t,t}(x,0)$, etcetera. Assuming this series converges (which is beyond the scope of this article), we can substitute this series into **(13)**

and group powers of t.

$$\begin{aligned}
\frac{\partial s}{\partial t} - H(s)\tau\frac{\partial^3 s}{\partial x^2 \partial t} + \ldots &= 0 \\
\sum_i^\infty \frac{P_{i+1}}{i!}t^i - \tau H(\sum_i^\infty \frac{P_i}{i!}t^i)\sum_{i=1}^\infty \frac{P''_{i+1}}{i!}t^i + \ldots &= 0 \\
\sum_i^\infty \frac{1}{i!}(P_{i+1} - \tau H(a)P''_{i+1} - G_i)t^i &= 0, \qquad \text{and thus,} \\
P_{i+1} - \tau H(a)P''_{i+1} &= G_i \qquad (49)
\end{aligned}$$

It can be seen that G_i only contains P_j with $j \leq i$, which makes equation **(49)** a differential equation in P_{i+1} if all P_j with $j \leq i$ are known. Moreover, since $P_0 = a$ and $P_1 = c\alpha e^{\alpha x}$ (with $c = 1 - f(a)$), it can even be shown that all $P_i(x)$ will be polynomials in terms of $\alpha^m x^l e^{n\alpha x}$ for certain m, l, n. Which means computer algebra systems such as Mathematica can solve the resulting differential equations (although clarity is not always achieved since the complexity of the terms involved quickly explodes).

Finally, note that this implies that $s^-_{t^n}(0)$ is a polynomial in α for every n. Moreover, note that $s^-(0)$ goes to zero for large τ but remains negative by definition. Also, $s^-(0) \to -\infty$ as $\tau \to 0$. If these transitions would be smooth we would for small t expect that $s^-_t(t) \sim -t^{-\lambda_1}$ and $s^-_t(t) \sim -t^{\lambda_2}$ for respectively small and large τ, with some non-negative (possibly infinite) λ_1 and λ_2. We actually fitted shifted/translated power-laws to $s^-_t(t)$ to test this, which were remarkably accurate for each separate τ, but further investigations into possible asymptotic solutions of $s^-(t)$ would be outside the scope of this article.

Now, with this in mind, and in accordance with our previous considerations with the coordinate transformation $t := \tau^{-1/2}t$, we would expect derivatives in the form of

$$s^-_{t^n}(0) = (-1)^n c_1 \alpha^k + P(\alpha) - c_2\alpha^n, \qquad (50)$$

For some nonnegative c_1, c_2, and where $k > n$, $P(\alpha) = o(\alpha^k)$ and $P(\alpha) = \omega(\alpha^n)$. Note that for even n it follows that $s^-_{t^n}(0)$ has *at least one zero*. This could imply possible critical behaviour, as we will see below.

Now, for $i = 2$, **(49)** reduces to

$$P_2(x) - \frac{1}{\alpha^2}P''_2(x) + H(a)J'(a)P''_1(x) + f'(a)P'_1(x) - \frac{H'(a)P'_1(x)^2}{\alpha^2 H(a)} = 0 \qquad (51)$$

With the help of Mathematica this differential equation can be solved, along with the boundary conditions $F_t(-\infty, 0) = 0$ and $F_t(0, 0) = 0$, and after greatly simplifying by grouping terms and letting $c = (1 - f(a))$ we get:

Theorem 9. *For all x we have*

$$\begin{aligned}
s_{t,t}(x, 0) &= -\frac{\alpha^2 c^2\left(2e^{2\alpha x} + e^{\alpha x}\right)H'(a)}{6H(a)} - \frac{1}{2}\alpha^2 c e^{\alpha x}(\alpha x + 1)\left(f'(a) + \frac{\alpha H(a)J'(a)}{h^-}\right) \qquad (52) \\
s^-_{t,t}(0) &= -\frac{\alpha^2 c^2 H'(a)}{6H(a)} - \frac{1}{2}\alpha^2 c\left(f'(a) + \frac{\alpha H(a)J'(a)}{h^-}\right) \qquad (53)
\end{aligned}$$

Note that the previously mentioned coordinate transformation $\hat{t} := \tau^{-1/2}t$ and $\hat{x} := \tau^{-1/2}x$ does *not* lead to an $s_{t,t}(x, t)$ independent of τ, as was the case for $s_t(x, t)$. Moreover, note the different behaviour of $s^-_{t,t}(0)$ for small or large values of τ. Since for large τ (and therefore small α) we have $s^-_{t,t}(0) \sim \tau$ and for small τ it follows that $s^-_{t,t}(0) \sim \tau^{3/2}$, illustrating the different regimes

for different τ, and corresponding with our previous prediction.

We can even pinpoint the exact τ such that $s^-_{t,t}(0) = 0$. Solving this equation and incorporating the definition of H, results in an equation entirely dependent on a (through $k_{rn}(a)$ and $k_{rw}(a)$) and the capillary number N_c:

$$\tau_c = \frac{9\frac{H(a)}{(h^-)^2}J'(a)^2}{\left(3f'(a) - (1-f(a))\frac{H'(a)}{H(a)}\right)^2}$$

$$\frac{\tau_c}{N_c} = \frac{9k_{rn}(a)f(a)J'(a)^2}{\left(3f'(a) - (1-f(a))\frac{(k_{rn}(a)f(a))'}{k_{rn}(a)f(a))}\right)^2} \tag{54}$$

$$\tag{55}$$

Note that the parameter transformation $\tau := c_1\tau$, $N_c := c_1 N_c$ for any constant c_1 corresponds to a simple coordinate transformation $t := c_1 t$, $x := c_1 x$, which illustrates the possible critical role of τ_c/N_c.

Finally, it appears that for our functional dependencies $\tau_c(a)/N_c$ does not vary greatly over the interval $[0, 1]$, as can be seen from Figure 15. For $a \geq 0.1$ τ_c does not change more than a factor of 3, and reaches a maximum at $9/64 \approx 0.14$. This would suggest that the observed phenomena would hold for roughly the same order of magnitude in τ across a wide range of a, which is exactly what we will see in our second example. Also, note that for $a = 0.4$ it holds that $\tau_c = 0.07$, corresponding roughly to the yellow simulation with $\tau = 0.05$.

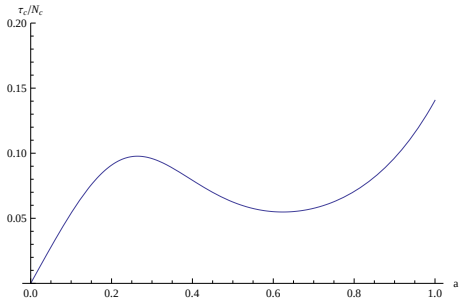

Figure 15: Critical value τ_c as a function of a and N_c

5.2.2.3 Behaviour at interface for $h^+ = \sqrt{0.1}$

The behaviour for $\boldsymbol{h^+ = \sqrt{0.1}}$ was already briefly mentioned and shown in Figure 12, with plots at different times for the entire interval $[x_l, x_r]$. Now we consider the behaviour of $s^{\pm}(t)$ and $p_c(t)$ at the interface, see Figure 16.

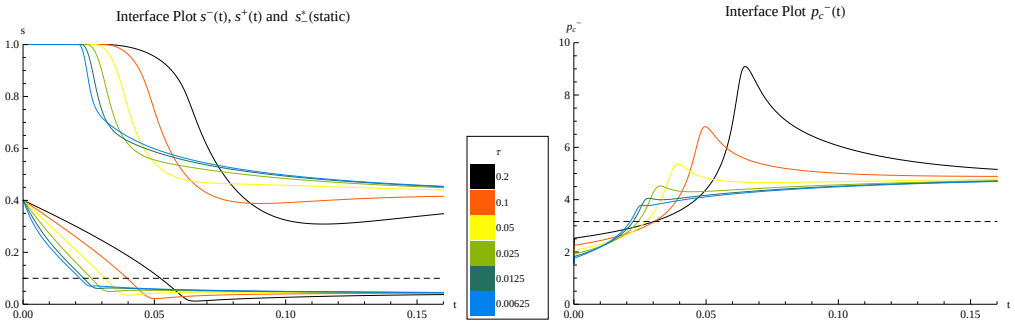

Figure 16: Interface Plots of $s^{\pm}$ and p_c, including s^*_-(static) and $\bar{p}^+_s = J(1)/h^+$

Before we investigate possible scaling effects similar to the one seen in the previous section, let us look more closely at the evolution of $s^-(t)$ and $s^+(t)$. Firstly, note that the limit value of s^+ is roughly equal to $s^+(\infty) = 0.4$, since as the oil-water boundary progresses and the flux decreases, the the slope of the flux would go to zero for an infinite interval - forcing $F_0 = F(-\infty)$ and therefore $s^+(\infty) = s(\infty, t) = 0.4$. Thus, s^- eventually goes a number roughly equal to 0.04, since $J(0.04)/h^- = J(0.4)/h^+$, but the finite interval might change these values a little bit.

Now, at first, $s^-(t)$ looks strikingly similar to the scenario with $k^+ = 0$ (where $F(0,t) = 1$ for all t), and for large tau even well after the pressure discontinuity is broken and $s^+(t)$ is falling. Then, after passing the $s^*_{-,s} = 0.1$-mark (at which point the pressure would become continuous for the equilibrium case $\tau = 0$), $s^-(t)$ changes course and eventually goes towards its limit value. The remainder of this section is to investigate this evolution more closely and explain these phenomena.

To do so we introduce the following sequential points in time, which will be represented by dots on the next interface plots: the time at which the pressure discontinuity is broken t_b (gray dots or the line $p_c = J(1)/h^+$), the time t^* at which s^- reaches its equilibrium counterpart (blue dots or the line $s = s^*$), and the time t_Δ at which the quantity $[\tau s_t]$ (whose role was discussed in the previous chapter) reaches a minimum (black dots) - more on that later. Note that for $\tau = 0$ these times would all converge. Now consider the interface plots of $s^{\pm}$, $s^{\pm}_t$ and p^- with the various points of time interlaced, as shown in Figure 17. Moreover, the scenario for $k^+ = 0$ is represented by the dashed lines in the interface plot for s^-_t.

First note that the ordering of t_b (and thus $s^-_{t_b}$ and $p^-_c(t,b)$)) for the various τ is completely determined by the case with $k^+ = 0$, and follow from our previous results. Secondly, in the figure for $s^-(t)$ one can clearly see the striking comparison between the case for $k = 0.1$ and $k^+ = 0$, which diverge from each other right about the time t^* the static s^* is reached (the blue dots). This is far from obvious. From the moment the capillary pressure becomes continuous the two scenarios are no longer equal and are free to diverge. Moreover, it means that $s^-(t)$ is largely *independent* from k^+ until time t^*.

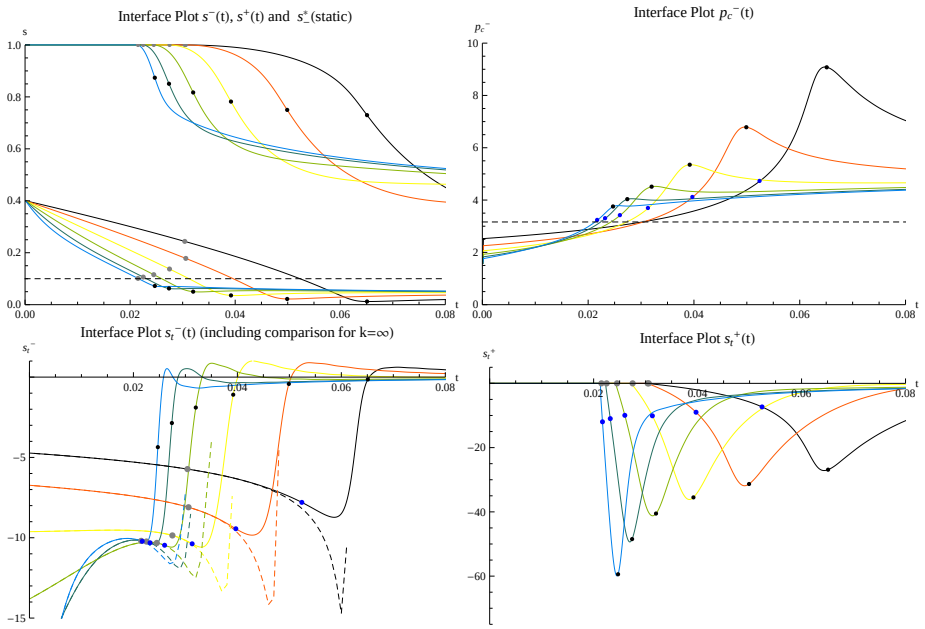

Figure 17: Interface plots with times t_b(gray), t^*(blue) and t_Δ (black)

One possible reason for the delay is that the flux F_0 decreases quite slowly (in all honesty, the apparent behaviour was first thought to be programming error when incorporating the extended pressure condition which hypothetically would force the flux to remain 1 - before it appeared to be otherwise). Note that $s_t^+(t_b) = 0$, in contrast to the equilibrium case. This is because at time t_b, the pressure has become continuous, so $J(s^-(t_b))/h^- - \tau s_t^-(t_b) = J(1)/h^+$, but since $s^-(t)$ is smooth this also means that $J(s^-(t_b))/h^- - \tau s_t^-(t_b) = J(s^+(t_b))/h^+ - \tau s_t^+(t_b)$, and our result follows. Now, since $f'(1) = 1$, it follows that $F_{0,t} = 0$ and $F_{0,t,t} = 0$, with only the third derivative in time being non-zero. As an example, consider Figure 18 for the case $\tau = 0.2$.

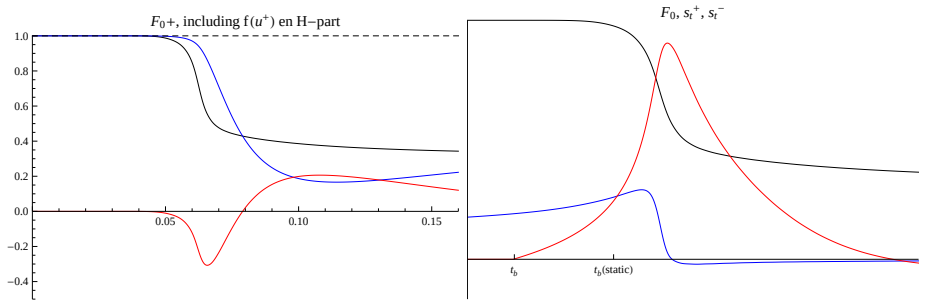

Figure 18: Plots of both the flux $F_0(t)$, compared with the evolution of (rescaled) $s_t^-(t)$ and $s_t^+(t)$, for $\tau = 0.2$

It can be seen that F_0 dóes begin to decrease at t_b, but incredibly slow. However, this can not explain why the flux rapidly decreases only after passing time t^*. A possible clue lies in the comparison between $s^-(t)$ and the dynamic counterpart of s^*, namely $s_-^*(t)$. Consider Figure 28. Firstly, $s^-(t)$ seems strictly bounded from below by $s^-_{k^+=0}(t)$ - note that if the formulas for $k^+ = 0$ were changed with $F_0 < 1$ it would force $0 > s_t^-(0) > s^-_{t,k^+=0}(0)$, which would help explain this

ordering. Moreover, remember that $s^-(t) \leq s^*_-(t)$ by definition when the pressure is continuous. Although $s^*_-(t)$ is defined by both $s^-(t)$ this would border on the verge of circular reasoning, but the picture is quite clear: $s^-(t)$ would 'stray too far' from $s^-_{k^+=0}$, the pressure would rapidly become discontinuous, in which case the boundary condition reverts $F_0(t) = 1$ again and $s^-(t)$ would continue on the course set by $s^-_{k^+=0}$. However, this does not yet explain whý $s^-_{k^+=0}(t)$ and $s^*_-(t)$ remain so close to begin with.

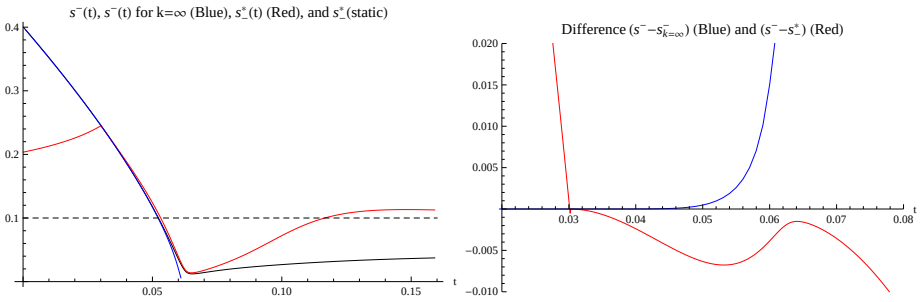

Figure 19: Comparison $s^-(t)$ with $s^*_-(t)$ and $s^-(t)$(with $k^+ = 0$

A hint to the final piece of the puzzle lies in the results of the previous chapter. Recall the behaviour of $[\tau s_t]$, and the example shown in which $s^+_e(t)$ catches up with $s^+(t)$, and that we observed that $[\tau s_t]_t < 0$ and $[\tau s_t]_{t,t} < 0$ while $[\tau s_t] > 0$ and the pressure was continuous. Also remember that when the pressure is continuous it holds that

$$\frac{J(s^-_e)}{h^-} - \frac{J(s^-_e)}{h^-} = \frac{J(s^+)}{h^+} - \frac{J(s^-)}{h^-} = [\tau s_t]. \tag{56}$$

Now suppose it is possible to prove our observation for certain restrictions, for example $s^+_t < 0$ and (and therefore $s^-_t < 0$, since $[\tau s_t] > 0$) and $s^-_{t,t}(t_b) < 0$, which could be forced by the flux condition for our initial saturation. Moreover, note that $0 < s^-_e < s^* = 0.1$ and $[\tau s_t] = 0$ if $s^- = s^-_e$. Then the observed behaviour of $[\tau s_t]$ would mean that s^- would go to s^+_e more and more rapidly (aka $[\tau s_t]_{t,t} < 0$) until it overshoots $s^+_e \approx s^*$ (in which case $[\tau s_t] > 0$) and eventually decays to s^+_e again. However, as $s^-(t)$ is bound from below by the slightly concave but nearly straight $s^-_{k^+=0}$, $s^-(t)$ can not diverge much from $s^-_{k^+=0}$ *until* $[\tau s_t]$ has switched signs (and roughly $s^- < s^*$). Which is exactly what we observe. As an example, consider the interface plot for $[J(s)/h]$ in Figure 29 for our various τ and compare its behaviour with our hypothesis.

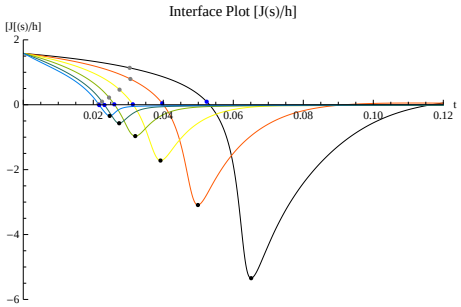

Figure 20: Interface Plot of $[J(s)/h]$

The times t_Δ are also derived from this Figure, since at these points $[\tau s_t]$ are minimized. The relation between these extrema and s^- and s^+ can be inferred but we will omit these considerations for the sake of clarity. Moreover, note that a more complete argument would need to place

explicit bounds on $[\tau s_t]_t < 0$ and $[\tau s_t]_{t,t} < 0$, incorporating the flux condition and the initial saturation.

As a final observation before we consider scaling behaviour, note that eventually $[\tau s_t]$ (and thus s^-, else this would not be possible) switches signs again for some τ. This is related to the fact that $s^-(t)$ seems to move slightly upward some time after t_Δ (increasing towards $s^-(\infty) = 0.04$) and moves slightly down towards 0.04 for other τ. The division seems to be the same as the critical behaviour noted previously. However, this has some peculiar consequences. Interpolating between these values would mean there is some τ^* (possible on the same scale as the τ_c considered previously) at which either $s^-(t)$ is discontinuous in τ for all $t > t^*$ for some t^*, ór it would follow that $s^-(t) = 0.04$ for all $t > t^*$ for some t^*. Either way, the result is a non-analyticity. Investigating this is beyond the scope of this article, but it does begs the question if the behaviour truly displays criticality, i.e. non-analyticities for some τ^*.

5.2.2.4 Scaling effects for $h^+ = \sqrt{0.1}$

First we consider the possible scaling for $s^-(t)$. Inspired by our previous analysis and Figure 14, we find that the same scalings give the best fit, see Figure 21. Since $s^-(t)$ and $s^-_{k^+=0}(t)$ do coalesce for quite a long time (until t^*), we would expect so. Still, the scaling for $t := \tau^{-3/8}t$ is even more clear now, showing that $t^* \sim \tau^{3/8}$ very accurately for $\tau > \tau_c$ and quickly diverges for $\tau < \tau_c$.

It is possible that for even larger τ the scaling $t := \tau^{-1/2}t$ becomes more accurate instead of $\tau^{-3/8}$. Remember that $s^-_{t,t}(0) \sim \tau$ for large τ and $s^-_{t,t}(0) \sim \tau^{3/2}$ for small τ, which if $s^-_{t,t}$ is representative for higher derivatives would lead us to expect scaling in time in the form of $t^* \sim \tau^{1/2}$ and roughly $t^* \sim \tau^{3/4}$ for respectively large and small τ. Remember that the value 3/4 can vary according to the higher derivatives, but the value 1/2 does not - as it linked to the previously mentioned coordinate transformation for large τ. However $3/8 < 1/2$ while we would expect a value between 1/2 and about 3/4. A possible reason could be the pole structure of $s_{t^k}(0)$ for even k, since a possible measure of the instantaneous exponent would be $\frac{\partial/\partial\tau(\log s_{t^k}(0))}{\partial/\partial\tau(\log\tau)}$. In the case of $s_{t,t}(0)$ this would imply a scaling smaller than 1/2 for $\tau > \tau_c$ (at some points even switching signs for τ very near τ_c), and a larger scaling than about 3/4 for $\tau < \tau_c$.

However, remember that for $\tau < \tau_c$, s_t converged to roughly the same point, throwing mud in the possibility of any scaling and begging new questions. However, further investigation is beyond the scope of this article.

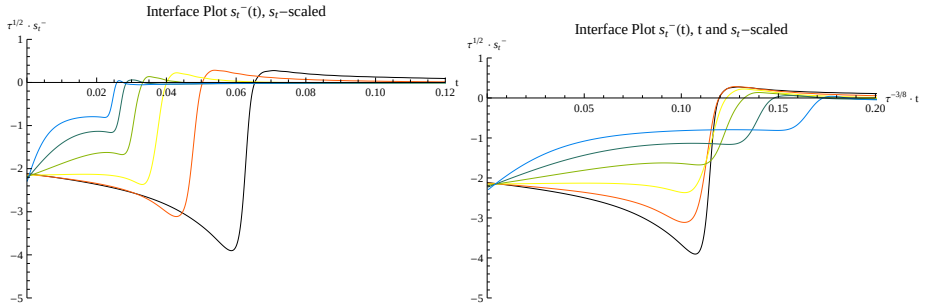

Figure 21: Interface Plots for s_t^-, scaled with $s_t^- := \tau^{1/2}s_t^-$ and $t := \tau^{-3/8}t$

Now, consider $s^+(t)$, which was obviously rather uninteresting in the case for $k^+ = 0$. For the case $k^+ = 0.1$, see Figure 22. First, note that for the best fit $s^+(t)$ was scaled by a factor $\tau^{1/4}$ instead of $\tau^{1/2}$. Although we already noted that we would expect a smaller exponent than $1/2$ for $\tau > \tau_c$, the difference is quite large and even seems to hold roughly for $\tau < \tau_c$. However, the best scaling for time was still $\tau^{-3/8}$ for $\tau > \tau_c$. Apparently the scalings for the general shape seem to hold quite consistently for large τ - and linked to this, the various key points in time: t_b, t^* and τ_Δ.

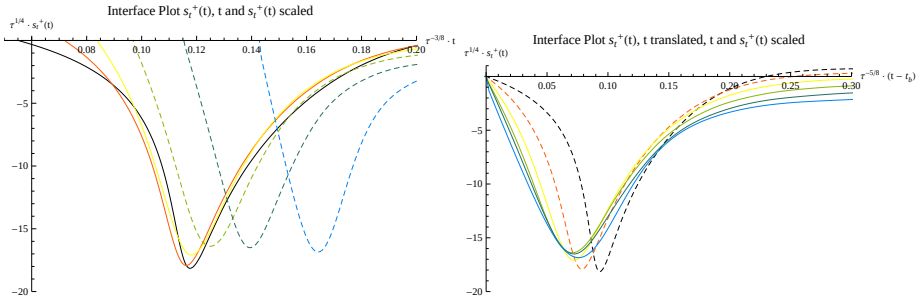

Figure 22: Interface Plots for s_t^+, with different appropriate scalings for $\tau > \tau_c$(left) and $\tau < \tau_c$ (right)

Secondly, there seemed to be no accurate scaling for $\tau < \tau_c$ in this case, *except* when the time was translated from the breaking point t_b (see again Figure 22) and scaled by $\tau^{-5/8}$. Note that $s^+(t_b) = 0$ by definition, but the resemblance is still quite remarkable, especially when compared to to the non-translated version (left). A possible explanation is to remember that for small τ the breaking points t_b seemed to converge to a single value instead of going to zero, which coincided (coincidentally!) in our example with the time $s^-(t)$ had already converged for small τ. Any possible scaling would have to start from that point, and since $s^-(t)$ would be roughly the same, s^+ (which is bound to $s^-(t)$ by the pressure condition after t_b) could be subject to possible scaling. However, this does not explain why the scaling is so accurate.

Now, we should be careful not to indulge in too much ad hoc scaling or explanations, but interesting pictures emerge. Instead of a smooth transition there seem to be separate scaling regimes for $\tau < \tau_c$ and $\tau > \tau_c$, with a very sharp division. Additionally, the scaling for $\tau < \tau_c$ means that as $\tau \to 0$, possible infinities would arise for $s_t^-(t)$ and $s_t^+(t)$, meaning that the transition from the non-equilibrium case to the equilibrium case is not smooth either. In this example it does not even seem to converge to what we would expect for $\tau = 0$ (which would lead to a discontinu but finite $s^+(t)$ around t_b), but since this example is only compatible with the flux condition for $\tau > 0$ it is hard to speculate. It did provide us however with valuable insight. Now, we will continue with our second example, concerning a oil-water wavefront. Since we can not rely on analysis as much as for this case, we will rely on these derived insights and try to draw comparisons from there.

5.2.3 Oil-Water Front

For this example we use the initial saturation shown in Figure 23, with the mesh included for completeness. Our program does not handle discontinuities very well, and therefore we modeled the initial saturation after what was seen for the equilibrium case simulated in [3]. Moreover, it is undefined for $s = 0$, which is why $s^- = 0.01$ for the part that is modeled after a medium that is fully saturated with oil. Thus, the boundary condition at x_l is $u_l = 0.01$. Beside u_l, the parameters for this example are the same as for the horizontal front shown in the previous section.

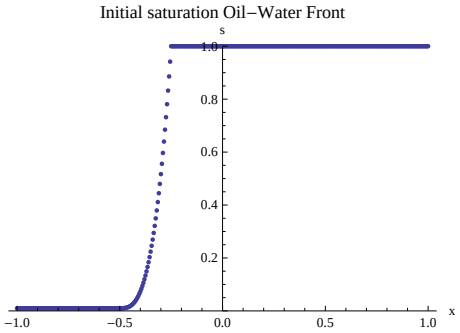

Figure 23: Initial saturation

Now, first consider the flow over the entire interval at various points in time, as shown in Figures 24 and 25. On the face of it we see the same kind of inversions and pressure bubble as shown in Figure 12. Although, note that for large τ the free boundary seems to lag the others, and converges as $\tau \to \infty$. The boundary speeds are actually not that very far apart, but there seems to be a small delay in the transition from the initial saturation to a sort of travelling wave, and this delay is larger for small τ.

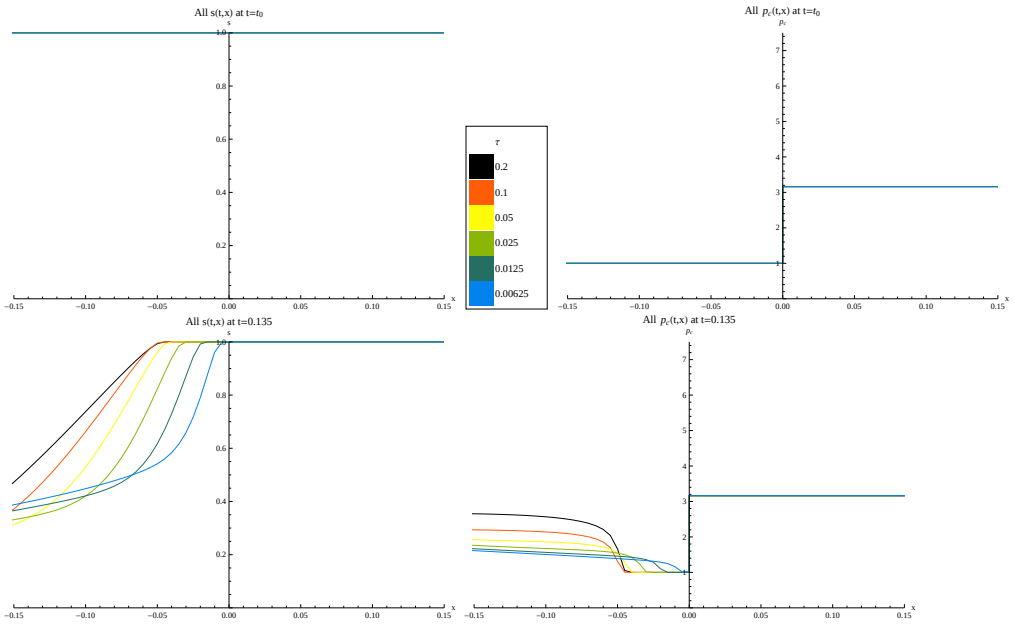

Figure 24: Plots of both $s(x,t)$ and $p_c(x,t)$ for various t (part a)

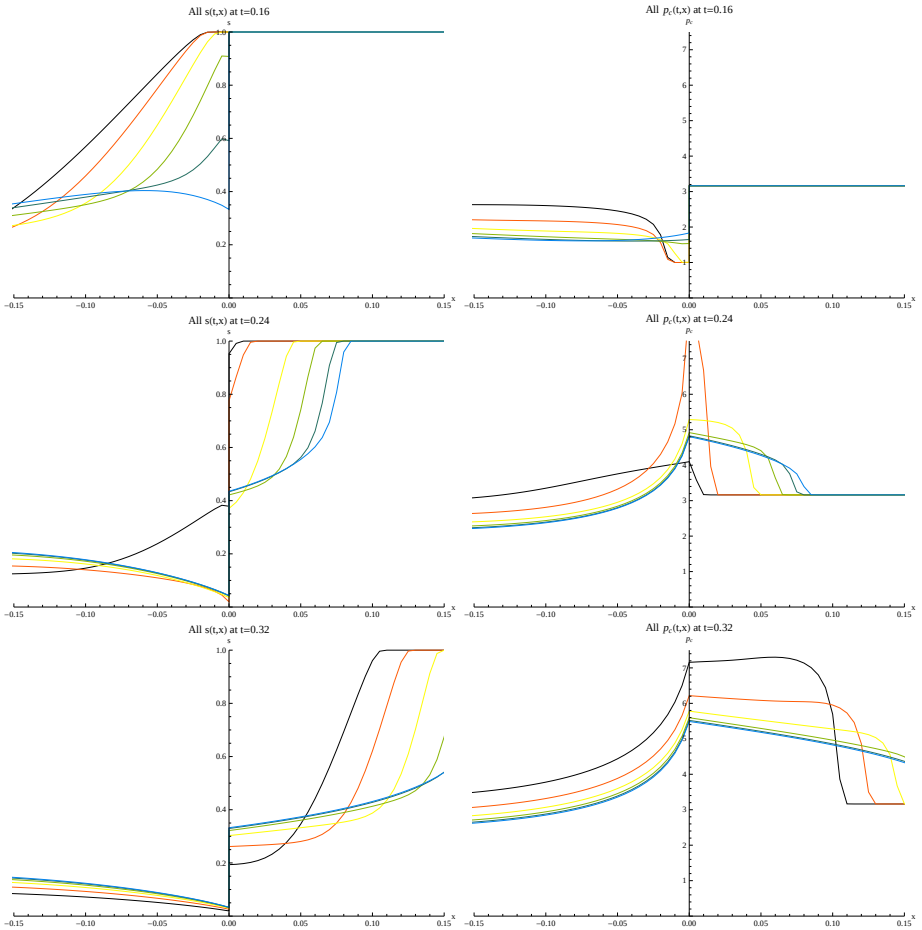

Figure 25: Plots of both $s(x,t)$ and $p_c(x,t)$ for various t (part b)

However, we will not try to investigate the intricacies of dynamic flow over the entire interval. For a thorough treatise on traveling waves for $\tau > 0$ one should consult [2]. Our focus lies on the behaviour around the interface, but the observation about the free boundary does pose some problems, as we will see below. Consider for example the Interface Plots for $s^{\pm}(t)$ and $p_c^-(t)$, as shown in Figure 26.

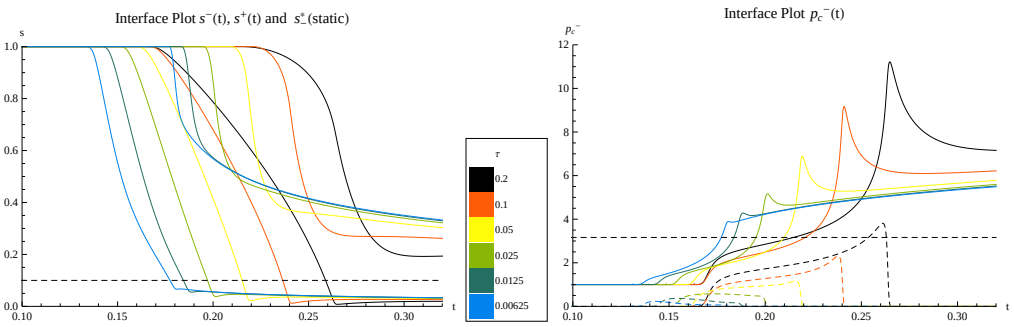

Figure 26: Interface Plots for $s^{\pm}(t)$, and $p_c^-(t)$

While there are interesting similarities and differences between this case and the one from the previous section, the delay of the free boundary does make it harder to discern, imposing a extra translation in t. This is also very clear in the evolution of $s^-(t)$, which will be shown later on. Moreover, note that since the delay converges as $\tau \to \infty$ instead of scaling with τ, one could not hope the kind of clear scaling behaviour shown previously.

Therefore, we quantify this delay by the time t_h at which the free boundary hits the interface, and translate all interface plots accordingly. Moreover, we will again make use of the previously introduced parameters t_b (gray dots or the line $p_c^- = J(1)/h^+$), t^* (blue dots or the line $s^- = 0.1$), and t_Δ (black dots), which correspond respectively to the time the discontinuity is broken, the time $s^-(t)$ reaches $s^* = 0.1$ (the equilibrium for $s^+ = 1$), and the time at which $[\tau s_t]$ is minimized. Now consider the translated interface plots, shown in Figure 5.2.3.

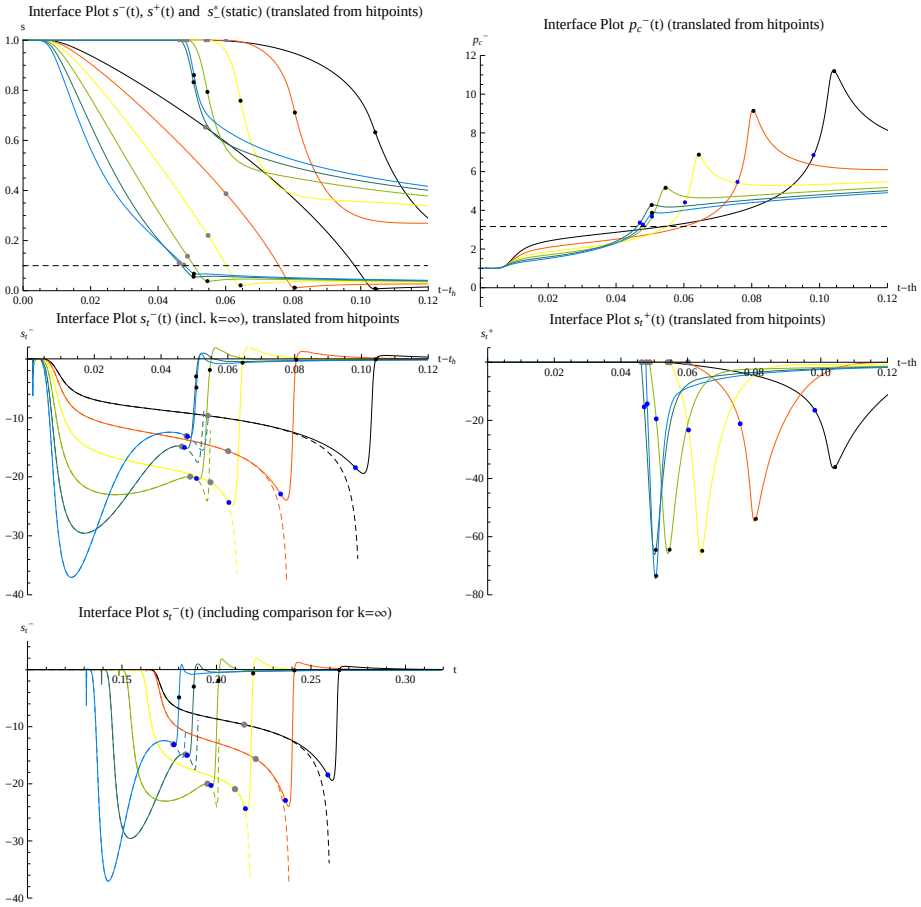

Figure 27: Interface Plots for $s^\pm(t)$, $s_t^\pm(t)$ and $p_c(t)$, translated from hitpoints t_h

Note the striking similarities between Figures 5.2.3 and 17. Apart from s^- starting at 1, the example with the horizontal front shown in Figure 17 seems as if as it a cropped version from Figure 5.2.3, starting at $t - t_h = 0.02$, although with a bit more pronounced shapes. The evolution in time follows the same principles: first $s^-(t) = s^-_{k^+=0}(t)$ in the interval $[t_h, t_b]$, then they nearly coincide (although less stringently than in the previous section, as will be shown below) while $s^+(t)$ is dropping, until (or just before) s^- finally dips below s^*_- at time t^*, and $s^-(t)$ and $s^+(t)$ make a swerve at t_Δ and slowly continu either upwards or downwards. Note that in this example the runtime is too short to make a prediction for $s^0(\infty)$ and $s^+(\infty)$, and the great disparity between u_l and u_r might have influence on these values. However, this is beyond the scope of this article.

Moreover, we see the same critical behaviour in s_t^- as before, both in the sharp division between the basic shape of s_t^- for various τ, and the sign of the slope of s^- after t_Δ. Note that $\tau_c(a)$ as defined in the previous section falls in the interval $[0.07, 0.014]$ for $a \in [0.4, 1]$. Since $\tau_2 = 0.25$ and $\tau_0.05$ this would explain why the division between the various τ is equal to our previous section. Finally, although τ_c is in this case apparently not clearly defined, in the remainder of the section we will use the shorthand $\tau > \tau_c$ for simplicity. Further investigation in the variation for τ $[0.07, 0.014]$ would pose a interesting problem however.

Additionally, in studying the shape of $s(x,t)$ we observed that for every τ the slope of $s(x,t)$ at the interface would at one point be zero before $s^-(t)$ would drop further, and that this happened at a lower $s^-(t)$ for higher τ. Now suppose that the point $s^-(t)$ at which the slope is horizontal for a certain τ is representative for its critical behaviour, being approximated by a small horizontal front with $a = s^-(t)$. Than this would mean that the evolution of $s^-(t)$ would be similar at this point to the previous example - but with a higher for high τ. Now remember that in our previous example the value at which $s^-(t)$ would briefly converge for $\tau < \tau_c$ was roughly equal to $s^-_{t,\tau_c}(0) = (f(a) - 1)\tau_c$. Then, since τ_c does not change much for not too small a, this would mean that in our example $s^-(t)$ would briefly converge to $s^-(t) \sim (1 - f(a_\tau))$. For lower τ this implies that $s^-(t)$ would briefly converge to a negative but higher value (or smaller in absolute terms), which is exactly what we see in the evolution of $s^-(t)$ as shown in Figure . Of course, this argument relies on a great similarity for different a and different shapes of the initial saturation, which we can not prove in this article - yet which we can try to illustrate, as shown above and in the remainder of this section.

As was mentioned previously, $s^-(t)$ does not diverge much from $s^-_{k^+=0}$ until t^*, although it diverges earlier than in our previous section. Inspired by our previous results, we revisit both the distance $|s^-(t) - s^*_-(t)|$ and $|s^-(t) - s^-_{k^+=0}(t)|$, as shown in Figure 28. One can see that although the differences are still very small, the distance $|s^-(t) - s^*_-(t)|$ is quite large compared to $|s^-(t) - s^-_{k^+=0}(t)|$. One could ask if for very large τ these distances would grow larger, putting a dent in our general argument that $s^-(t)$ is so close to $s^-_{k^+=0}(t)$ because diverging too much would rapidly break the pressure continuity, which is somehow prevented by the flux condition. Therefore, as we noted already, a more complete argument would need to make the restriction the flux condition places on s^+ more explicit (assuming a certain shape of $s(x,t)$).

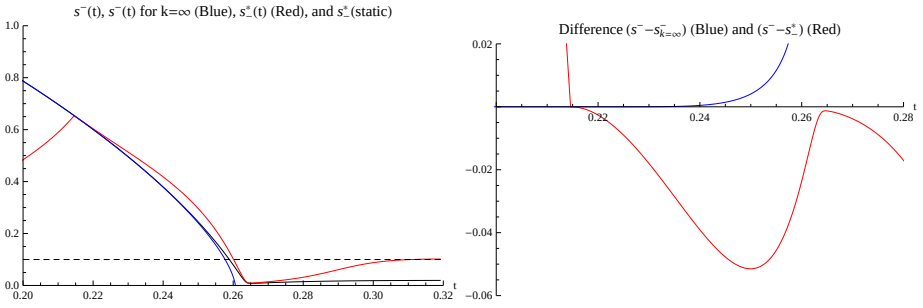

Figure 28: Comparison $s^-(t)$ with $s^*_-(t)$ and $s^-(t)$(with $k^+ = 0$

Finally, consider Figure 29 where we show the evolution of $[\tau s_t](t)$ (equal to $[J(s)/h]$ when the pressure is continuous), whose significance was already mentioned. Again we see that $[\tau s_t]_t < 0$ and $[\tau s_t]_{t,t} < 0$ as long as $[\tau s_t] > 0$, after which it overshoots and reverts again, never crossing zero again unless $s_t^- = s^+ = 0$. Although we could not prove all of this statement, as was mentioned in Chapter 4, it does strengthens the case that for certain restrictions there is more information to be elicited than we have been able to so far. However, this is of course beyond the scope of this article.

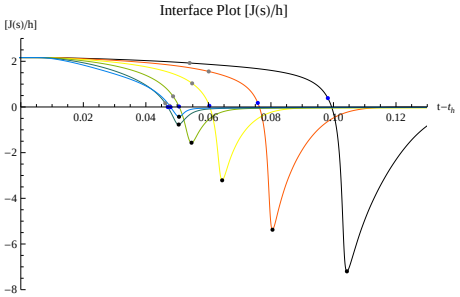

Figure 29: Interface plot of $[J(s)/h]$

Scaling effects

As we mentioned previously, the variation in the hitting time t_h for the various τ made investigation more difficult, and would prevent possible scaling. An an illustration, consider Figure 30, where the difference is quite clear. However, when we do translate for t_h, the same picture emerges as in our previous section: scaling $s^-(t)$ by a factor $\tau^(1/2)$ creates roughly the same result for small t and diverges quickly for $\tau < \tau_c$, and additionally, scaling $(t - t_h)$ by a factor $\tau^{-3/8}$ would make the general shapes for $\tau > \tau_c$ coincide. Again, note the remarkable rapid convergence of the point where $s_t^- = 0$ (roughly but not completely around time t_Δ).

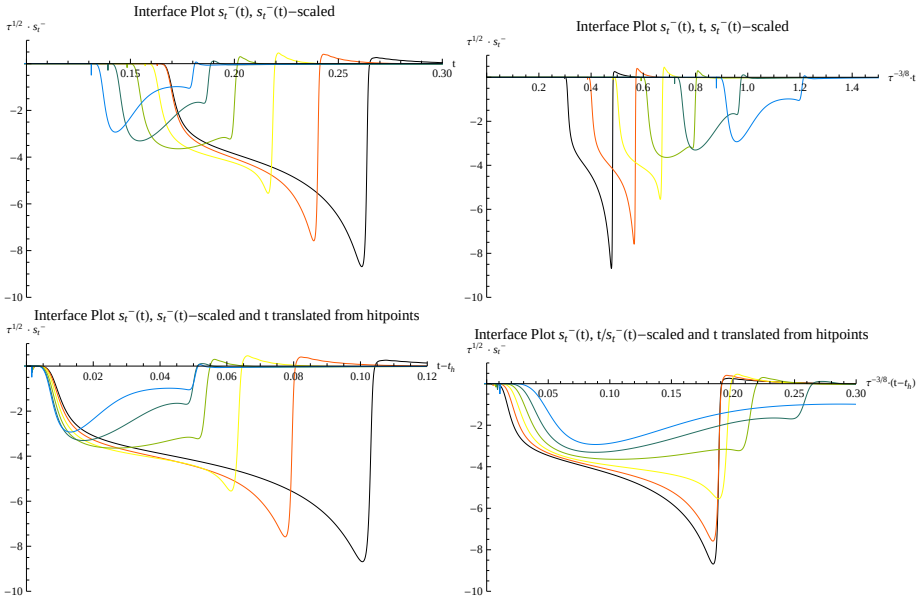

Figure 30: Scaling for $s^-(t)$

Now, when scaling s^+, we again see separate behaviour for $\tau > \tau_c$ and $\tau < \tau_c$, translating respectively from t_h, or from t_b - in accordance with the results on our horizontal wavefront. Although the scaling in t is exactly the same as before, it should be noted that the height of the peaks of $s^+(t)$ do not seem to scale for $\tau < \tau_c$, being roughly similar except for τ_6. Now it is possible that scaling would occur for very small τ (the peak for τ_6 is quite smaller than for τ_4 and τ_4, however we can not be certain given the data we have. A possible reason for this gap in scaling could be the different nature of $s^-(t)$ in comparison with our horizontal front, since $\tau_c(a_\tau)$ varies as was mentioned previously. It is possible these effects conflict with each other, muddying the similarity.

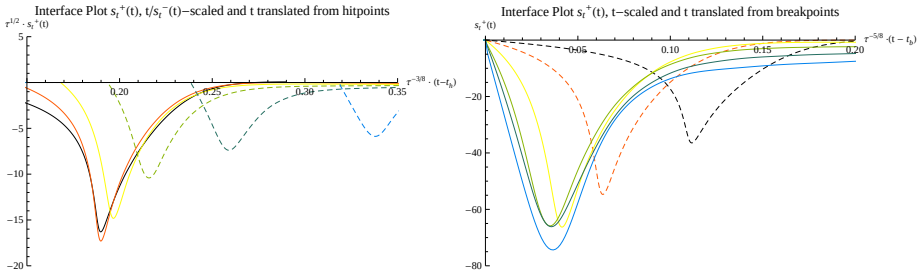

Figure 31: Scaling for $s^+(t)$

6 Conclusion

In the introduction we mentioned that we would like to make a modest starting point investigating the coalescence of a discontinuous capillary pressure over a material interface, and one depending on a dynamic parameter τ. It turned out however that this combination provided a extremely rich subject, which - at the cost of brevity - lead to several strands of questions, many of them still left unanswered. From these lines of inquiry various pictures emerged, as will be listed below.

First we investigated the possible well-posed form the extended pressure condition would take in the non-equilibrium case. Although we did not succeed in rigourously proving the resulting interface conditions by a regularization approach, we did provide some partial results. Moreover, we showed that the limiting behaviour of those neighborhoods of v_ϵ, with $v_\epsilon \to 1$ as $\epsilon \to 0$, are key to further advances.

Next, assuming the interface conditions, we analyzed its possible implications if either $s^-(t)$ or $s^+(t)$ were given. Beside showing existence and uniqueness, we provided results concerning the asymptotic behaviour. But more importantly, given certain conditions, we proved various relationships between $s^-(t)$ and $s^+(t)$ and their equilibrium counterparts $s_e^\pm(t)$ which would hold for all t - showing for example that $s_e(t)$ can only catch up with $s(t)$ instead of the other way around, if both are not equal to zero. We illustrated these results by numerically computing $s^+(t)$ for certain smooth $s^-(t)$.

Finally, we simulated two-phase flow on a entire interval, incorporating both the extended pressure condition and the flux condition. We found that over a range of τ there are essentially two different types of behaviour with a very sharp division around a certain critical τ_c, and that for both regimes there were appropriate scalings in powers of τ. In studying the abstract example of a piece-wise initial saturation we derived important analytical results supporting both the scaling and the display of criticality, and illustrated the striking similarities between this example and one with a more general oil-water wavefront.

As mentioned, every answer raised even more questions, but we hope that this research provides a first step in studying the interesting effects of a dynamic but discontinuous capillary pressure. Possible avenues include continuing the regularization approach, explicitly setting bounds on $[\tau s_t]$, investigating the possible non-analyticities that arise for τ_c, and studying further scaling effects for general initial saturations or for example traveling waves. However, the one scenario that is most enticing in the one with several interfaces, or its limit, a homogenization approach. The possible cancelling or amplifying effects of scaling, the independence of k^+ for certain instances, and the critical behaviour in τ would lead to very interesting repercussions on the resulting effective equations. All things considered, it is clear there remains a trove of interesting effects to be discovered, and we hope to have made a modest contribution along the way.

References

[1] C.J. van Duijn, *An Introduction to Conservation Laws: Theory and Applications to Multi-Phase Flow*, TU/e (2003), 127-132

[2] C.J. van Duijn, Y. Fan and L.A. Peletier, *Dynamic Capillarity in Porous Media - Mathematical Analysis*, Nonlinear Anal. Real World Appl. **14** (2013), 1361-1383

[3] C.J. van Duijn, J. Molenaar and M.J. De Neef, *The Effect of Capillary Forces on Immiscible Two-Phase Flow in Heterogeneous Porous Media*, Transp. Porous Media **21** (1995), 71-93

[4] C. J. van Duijn, A. Mikelić and I. S. Pop, *Effective equations for two-phase flow with trapping on the microscale*, SIAM J. Appl. Math. **vol. 62, No. 5** (2002), 1531-1568

[5] C.J. van Duijn, H. Eichel, Rainer Helmig, and I.S. Pop, *Effective equations for two-phase flow in porous media: the effect of trapping on the microscale*, Trans. Porous Media **69** (2007), 411-428

[6] R. Helmig, A. Weiss and B.I. Wohlmuth, *Dynamic capillary effects in heterogeneous porous media*, Comput. Geosc. **11** (2007), 261-274